those with sporadic ALL (non-DS patients; Buitenkamp et al., 2014). DS-ALL patients also experience increased morbidity and mortality in association with chemotherapy (Buitenkamp et al., 2014). Thus, more effective and less toxic treatments, such as targeted therapies, are needed for these patients.

The cytokine receptor-like factor 2 (*CRLF2*) gene encodes a protein that plays a role in cellular proliferation via activation of the JAK-STAT signaling pathway. Overexpression of *CRLF2* is observed in approximately 50–60% of DS-ALL patients in Western countries (Mullighan et al., 2009; Russell et al., 2009; Hertzberg et al., 2010). In most of these patients, *CRLF2* overexpression is associated with interstitial deletions of the pseudoautosomal regions (PAR1-IDs) of the sex chromosomes, resulting in the *P2RY8-CRLF2* fusion. Less frequently, translocations between the immunoglobulin heavy chain locus (*IGH*) and PAR1 that result in the *IGH-CRLF2* rearrangement are associated with *CRLF2* overexpression. *JAK2* mutations and *CRLF2* overexpression are thought to act cooperatively in leukemogenesis, and activating *JAK2* mutations are observed in approximately 20% of DS-ALL patients (Bercovich et al., 2008; Gaikwad et al., 2009; Kearney et al., 2009). Mutations in *JAK1*, *CRLF2*, and interleukin-7 receptor-α (*IL7R*) are found in less than 10% of DS-ALL patients (Hertzberg et al., 2010; Blink et al., 2011; Shochat et al., 2011). Although the CRLF2-JAK signaling pathway is considered a potential therapeutic target, the incidence rates of these genetic alterations have not been established for Asian patients with DS-ALL.

In contrast to the mechanisms discussed above, the frequencies of gene deletions involved in the pathogenesis of B-cell precursor ALL (BCP-ALL) in DS-ALL patients are similar to those in non-DS ALL patients (Hertzberg et al., 2010; Loudin et al., 2011). *IKZF1* deletions have been detected in approximately 20–30% of DS-ALL patients, and are associated with a poor outcome (Buitenkamp et al., 2012; Patrick et al., 2014). The initial report of frequent *BTG1* deletions in older male DS-ALL patients (29%) was not confirmed in a subsequent study using a larger cohort (Lundin et al., 2012; Buitenkamp et al., 2013), and *EBF1* deletions have rarely been found in DS-ALL cases (Kearney et al., 2009; Hertzberg et al., 2010; Ensor et al., 2011; Loudin et al., 2011; Buitenkamp et al., 2012). The frequencies and clinical implications of these gene deletions in Asian DS-ALL patients also remain to be determined. Therefore, the goal of this study was to evaluate genetic alterations and their associated clinical effects in 38 DS-ALL patients of Japanese descent.

MATERIALS AND METHODS

Patients and Samples

This study was approved by the Ethics Committee of Hirosaki University Graduate School of Medicine, and all clinical samples were obtained with parental informed consent in accordance with the Declaration of Helsinki. Diagnostic bone marrow samples were obtained from 28 DS-ALL patients <20 years of age from 14 pediatric and/or hematology departments throughout Japan. These samples included frozen bone marrow cells ($n = 17$) and genomic DNA extracted from bone marrow specimens ($n = 11$). All patients were treated with curative intent according to various protocols between 1987 and 2011. Additionally, frozen bone marrow cells of 10 patients who were treated with the Japan Association of Childhood Leukemia Study (JACLS) ALL-97 or ALL-02 protocol between 1997 and 2007 were obtained from the JACLS investigators. The protocols were approved by the institutional review board of each participating institute, and written informed consent was obtained from the parents of all patients. The bone marrow samples of 25 unselected non-DS ALL patients who were treated at Hirosaki University Hospital between 2002 and 2010 served as controls for the *CRLF2* expression study. Genomic DNA was extracted from bone marrow cells with the QIAamp DNA Blood Mini Kit (QIAGEN, Venlo, The Netherlands), and total RNA was extracted with the RNeasy Plus Mini Kit (QIAGEN). Complementary DNA (cDNA) was prepared using the iScript cDNA Synthesis Kit (Bio-Rad Laboratories, Hercules, CA).

Clinical data of the first 28 patients were collected by a standardized questionnaire and included sex, age at diagnosis, initial white blood cell (WBC) count, cytogenetic and molecular genetic abnormalities, treatment protocol, and outcome. Data on the additional 10 patients were provided by JACLS.

P2RY8-CRLF2 Amplification and Mutation Analysis

Genomic polymerase chain reaction (PCR) and reverse-transcription polymerase chain reaction (RT-PCR) for the *P2RY8-CRLF2* fusion were performed using previously described primers (Mullighan et al., 2009; Harvey et al., 2010; Morak et al., 2012). All PCR products were directly

sequenced in both directions using the ABI PRISM BigDye Terminator Cycle Sequencing Ready Reaction Kit (Applied Biosystems, Foster city, CA) on an ABI PRISM 310 Genetic Analyzer (Applied Biosystems).

Genomic PCR and/or RT-PCR were performed for exons 12–18 of *JAK1*, exons 13–19 of *JAK2*, exons 11–15 of *JAK3*, exons 1–6 of *CRLF2*, and exons 5 and 6 of *IL7R* using previously described primers (Bercovich et al., 2008; Sato et al., 2008; Hertzberg et al., 2010; Shochat et al., 2011). All PCR products were directly sequenced in both directions.

Quantitative Real-Time PCR

Quantitative real-time PCR for *CRLF2* was performed using previously described primers (Yoda et al., 2010) and iQ SYBR Green Supermix (Bio-Rad Laboratories) on the Chromo4 Real-time PCR System (Bio-Rad Laboratories). Each sample was run in triplicate. The comparative Ct method was used to quantify relative mRNA expression levels using the endogenous control gene *GAPDH*.

Copy Number Determination

Multiplex ligation-dependent probe amplification (MLPA) was performed using the SALSA MLPA probemix P335-B1 ALL-IKZF1 to detect chromosomal deletions and/or duplications associated with ALL. Reactions were performed according to the manufacturer's instructions (MRC-Holland, Amsterdam, The Netherlands). Values <0.75 and >1.3 were considered indicative of deletions and amplifications, respectively (Schwab et al., 2010). PAR1-IDs were defined as *CSF2RA/IL3RA/P2RY8* deletions with normal or amplified *CRLF2*.

Statistical Analysis

Differences in the distribution of individual parameters among patient subsets were analyzed using the Fisher's exact test for categorized variables and the Mann–Whitney *U* test for continuous variables. Estimation of survival was performed using the Kaplan–Meier method, and differences were compared using the log-rank test. Event-free survival (EFS) was defined as the time from diagnosis to any event (induction failure, relapse, death, or second malignancy), and overall survival (OS) was defined as the time from diagnosis to death from any cause. *P*-values < 0.05 were considered statistically significant.

RESULTS

Clinical Characteristics of DS-ALL Patients

The clinical characteristics of the 38 Japanese DS-ALL patients are summarized in Table 1. Full clinical datasets were available for 34 patients, and sex, age, and treatment protocol data were available for 35 patients. The male to female ratio was 1.1:1, and the median age at diagnosis was 6.4 years (range, 2.2–19.1 years). The median WBC count at diagnosis was 16.5×10^9/l (range, 1.1–187.5×10^9/l), and 47% of patients were classified as high risk according to the National Cancer Institute (NCI) risk criteria. Recurrent cytogenetic abnormalities were found in six patients (16%): two with t(12;21)(p13;q22), two with high hyperdiploidy, one with dic(9;20)(p13;q11), and one with t(8;14)(q11;q32). With a median follow-up of 44.0 months (range, 2–221 months), estimated 5-year EFS and OS were 65.8 ± 9.3 and $70.9 \pm 9.0\%$, respectively.

P2RY8-CRLF2 and *JAK2* Mutations

The *P2RY8-CRLF2* fusion was identified in 11 patients (29%) by genomic PCR and/or RT-PCR (Table 1), 3 of whom had the newly discovered breakpoint 2.1 kb upstream of the *CRLF2* exon 1 (Morak et al., 2012). The *JAK2* R683G mutation was observed in six patients (16%; Table 1), consisting of the same single nucleotide substitution (c.2047A>G). These six patients also carried the *P2RY8-CRLF2* fusion. No mutations were found in *JAK1*, *JAK3*, *CRLF2*, or *IL7R* in any of the patients.

CRLF2 Expression

CRLF2 expression levels were compared among three patient groups: *P2RY8-CRLF2*-positive DS-ALL, *P2RY8-CRLF2*-negative DS-ALL, and non-DS ALL. RNA was available from 27 DS-ALL patients, including 7 *P2RY8-CRLF2*-positive and 25 non-DS ALL patients. The median *CRLF2* expression level in the *P2RY8-CRLF2*-positive DS-ALL patients was significantly higher than that in *P2RY8-CRLF2*-negative DS-ALL ($P = 0.001$) and non-DS ALL patients ($P < 0.001$; Fig. 1). No significant difference in *CRLF2* expression levels was observed between *P2RY8-CRLF2*-negative DS-ALL and non-DS ALL patients. When a *CRLF2* level $\geq$10-fold the median level in non-DS ALL patients was defined as overexpression (Harvey et al., 2010), 6 of 7 *P2RY8-CRLF2*-positive and 3 of 20 *P2RY8-*

TABLE 1. Clinical and Genetic Characteristics of DS-ALL Patients

Patient no.	Sex	Age (years)	WBC ($\times 10^9$/l)	NCI risk	Recurrent cytogenetic abnormality	EFS (months)	OS (months)	*P2RY8-CRLF2*	*JAK2*
1	F	4.5	46.5	SR	No	12+	12+	Positive	R683G
2	M	6.2	26.9	SR	No	30, relapse	87+	Positive	R683G
3	F	8.2	65.4	HR	No	38+	38+	Positive	R683G
4	F	3.4	3.7	SR	No	2, death in CR	2	Positive	R683G
5	M	2.7	27.2	SR	No	63+	63+	Positive	R683G
6	F	4.8	2.2	SR	No	9+	9+	Positive	R683G
7	M	4.4	2.1	SR	No	24, relapse	30	Positive	WT
8	M	15.0	187.5	HR	No	60+	60+	Positive	WT
9	F	4.2	1.9	SR	No	17+	17+	Positive	WT
10	NA	NA	NA	NA	NA	NA	NA	Positive	WT
11	F	15.8	2.0	HR	No	4, death in CR	4	Positive	WT
12	M	2.2	57.3	HR	No	85+	85+	Negative	WT
13	M	6.4	55.0	HR	No	50+	50+	Negative	WT
14	F	7.0	2.2	SR	No	49+	49+	Negative	WT
15	M	16.8	70.7	HR	No	0, IF	27	Negative	WT
16	M	11.4	9.0	HR	No	39+	39+	Negative	WT
17	NA	NA	NA	NA	NA	NA	NA	Negative	WT
18	M	11.2	1.1	HR	No	81+	81+	Negative	WT
19	F	8.1	4.5	SR	No	26+	26+	Negative	WT
20	F	4.5	107.5	HR	t(12;21)(p13;q22)	13+	13+	Negative	WT
21	F	4.8	108.9	HR	t(12;21)(p13;q22)	128+	128+	Negative	WT
22	M	2.8	10.9	SR	High hyperdiploidy	221+	221+	Negative	WT
23	M	6.7	10.5	SR	No	0, IF	51	Negative	WT
24	M	19.1	2.6	HR	No	60+	60+	Negative	WT
25	F	2.9	38.9	SR	No	76, relapse	128+	Negative	WT
26	M	4.8	51.2	HR	No	77+	77+	Negative	WT
27	F	9.7	44.9	SR	dic(9;20)(p13;q11)	63+	63+	Negative	WT
28	F	9.8	61.7	HR	t(8;14)(q11;q32)	52, relapse	56+	Negative	WT
29	M	7.3	13.6	SR	No	0, IF	20	Negative	WT
30	M	8.7	51.6	HR	No	0, IF	12	Negative	WT
31	F	17.2	47.3	HR	No	15+	15+	Negative	WT
32	M	13.6	13.2	HR	No	84, relapse	101+	Negative	WT
33	F	7.1	19.5	SR	No	14+	14+	Negative	WT
34	M	5.3	3.8	SR	High hyperdiploidy	61, relapse	64+	Negative	WT
35	NA	NA	NA	NA	NA	NA	NA	Negative	WT
36	F	6.4	3.9	SR	No	10, relapse	22	Negative	WT
37	M	4.8	NA	NA	NA	NA	NA	Negative	WT
38	F	6.3	3.0	SR	No	27+	27+	Negative	WT

WBC, white blood cell; NCI, National Cancer Institute; EFS, event-free survival; OS, overall survival; M, male; F, female; SR, standard risk; HR, high risk; CR, complete remission; IF, induction failure; WT, wild type; NA, not available.

CRLF2-negative DS-ALL patients exhibited *CRLF2* overexpression (9/27, 33% in total).

Copy Number Alterations of Genes Involved in BCP-ALL Development

A summary of the MLPA results is shown in Figure 2. DNA samples from 32 patients were available for analysis. PAR1-IDs were detected in eight patients (25%), all of whom were positive for *P2RY8-CRLF2*. In one patient with *P2RY8-CRLF2*, values for *CSF2RA/IL3RA/P2RY8* were lower than that for *CRLF2*, but the result did not meet the criteria of PAR1-IDs. *EBF1* deletions were found in five patients (16%), significantly more in *P2RY8-CRLF2*-positive than in *P2RY8-CRLF2*-negative patients (44% vs. 4%, $P = 0.015$). Conversely, deletions of *CDKN2A/B* and *PAX5* were common in *P2RY8-CRLF2*-negative patients (48 and 39%, respectively) but rare in *P2RY8-CRLF2*-positive patients (11% each), although the differences were not statistically significant ($P = 0.103$ and 0.210, respectively). Deletions of *BTG1* and *IKZF1* were detected in eight patients each (25%), and four and three of these patients had *P2RY8-CRLF2*, respectively. Deletions of

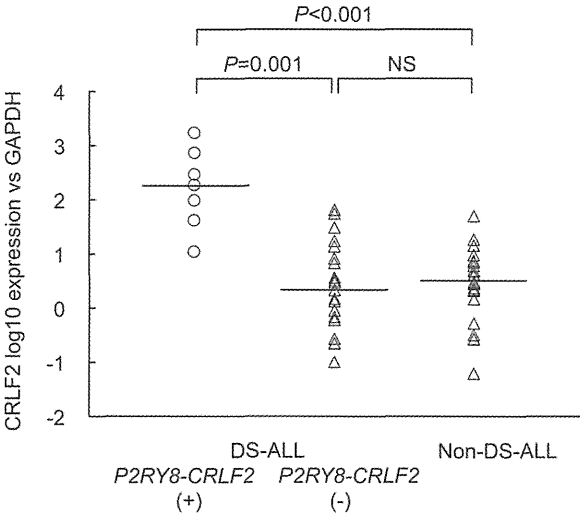

Figure 1. *CRLF2* expression in DS-ALL and non-DS-ALL. Open circles: DS-ALL patients with *P2RY8-CRLF2*; triangles: other patients; and horizontal bars: median *CRLF2* expression levels. NS, not significant.

ETV6 and *RB1* were found in 5 (16%) and 2 (6%) patients, respectively, all of whom were negative for *P2RY8-CRLF2*.

Association of Genetic Alterations with Clinical Characteristics

The distributions of sex, age at diagnosis, initial WBC count, NCI risk group, and recurrent cytogenetic abnormalities did not differ significantly between patients with and without each genetic alteration. The results for *P2RY8-CRLF2*, *BTG1*, and *IKZF1* are shown in Table 2. Of note, no *P2RY8-CRLF2*-positive patients had recurrent cytogenetic abnormalities. In patients with *BTG1* deletions, the male to female ratio was 1.0, and mean age was 4.8 years (range, 2.2–11.2). Estimated EFS and OS were not significantly different between patients with and without each genetic

Patient No.	*P2RY8-CRLF2*	*JAK2*	*PAR1*	*EBF1*	*BTG1*	*IKZF1*	*PAX5*	*CDKN2A/B*	*RB1*	*ETV6*
1	Positive	R683G								
2	Positive	R683G								
3	Positive	R683G								
4	Positive	R683G								
5	Positive	R683G								
6	Positive	R683G								
7	Positive	WT								
8	Positive	WT								
9	Positive	WT								
10	Positive	WT								
11	Positive	WT								
12	Negative	WT								
13	Negative	WT								
14	Negative	WT								
15	Negative	WT								
16	Negative	WT								
17	Negative	WT								
18	Negative	WT								
19	Negative	WT								
20	Negative	WT								
21	Negative	WT								
22	Negative	WT								
23	Negative	WT								
24	Negative	WT								
25	Negative	WT								
26	Negative	WT								
27	Negative	WT								
28	Negative	WT								
29	Negative	WT								
30	Negative	WT								
31	Negative	WT								
32	Negative	WT								
33	Negative	WT								
34	Negative	WT								
35	Negative	WT								
36	Negative	WT								
37	Negative	WT								
38	Negative	WT								

Deleted Not done

Figure 2. Copy number alterations of genes involved in BCP-ALL development. The deletion frequencies are 8/32 (25%) for PAR1, 5/32 (16%) for *EBF1*, 8/32 (25%) for *BTG1*, 8/32 (25%) for *IKZF1*, 10/32 (31%) for *PAX5*, 12/32 (38%) for *CDKN2A/B*, 2/32 (6%) for *RB1*, and 5/32 (16%) for *ETV6*.

TABLE 2. Association Between Genetic Alterations and Clinical Characteristics

	P2RY8-CRLF2			BTG1			IKZF1		
	Positive ($n = 10$)	Negative ($n = 25$[a])	*P*-value	Positive ($n = 8$)	Negative ($n = 23$)	*P*-value	Positive ($n = 7$)	Negative ($n = 24$)	*P*-value
Sex									
Male, *n* (%)	4 (40%)	14 (56%)	0.471	4 (50%)	13 (57%)	1.000	4 (57%)	13 (54%)	1.000
Female, *n* (%)	6 (60%)	11 (44%)		4 (50%)	10 (43%)		3 (43%)	11 (46%)	
Age, years									
Median (range)	4.7 (2.7–15.8)	7.0 (2.2–19.1)	0.165	4.8 (2.2–11.2)	7.1 (2.7–19.1)	0.21	8.7 (4.4–16.8)	6.3 (2.2–19.1)	0.228
WBC, $\times 10^9$/l									
Median (range)	15.3 (1.9–187.5)	16.5 (1.1–108.9)	0.345	48.9 (1.1–107.5)	13.6 (1.9–187.5)	0.47	44.9 (2.1–187.5)	20.2 (1.1–108.9)	0.603
NCI risk group									
SR, *n* (%)	7 (70%)	11 (46%)	0.270	3 (38%)	13 (57%)	1.000	4 (57%)	12 (50%)	1.000
HR, *n* (%)	3 (30%)	13 (54%)		5 (63%)	10 (43%)		3 (43%)	12 (50%)	
Recurrent cytogenetic abnormality									
Yes, *n* (%)	0 (0%)	6 (25%)	0.148	1 (13%)	5 (22%)	1.000	1 (14%)	5 (21%)	1.000
No, *n* (%)	10 (100%)	18 (75%)		7 (87%)	18 (78%)		6 (86%)	19 (79%)	
5y EFS									
% ± SE	48.0 ± 19.0	72.0 ± 10.2	0.394	80.0 ± 17.9	65.7 ± 11.0	0.155	47.6 ± 22.5	74.6 ± 10.3	0.207
5y OS									
% ± SE	64.0 ± 17.5	74.4 ± 10.2	0.348	100	68.6 ± 10.9	0.162	41.7 ± 22.2	83.8 ± 8.9	0.041

WBC, white blood cell; NCI, National Cancer Institute; SR, standard risk; HR, high risk; EFS, event-free survival; OS, overall survival.
[a]In one patient, data were only available for sex and age.

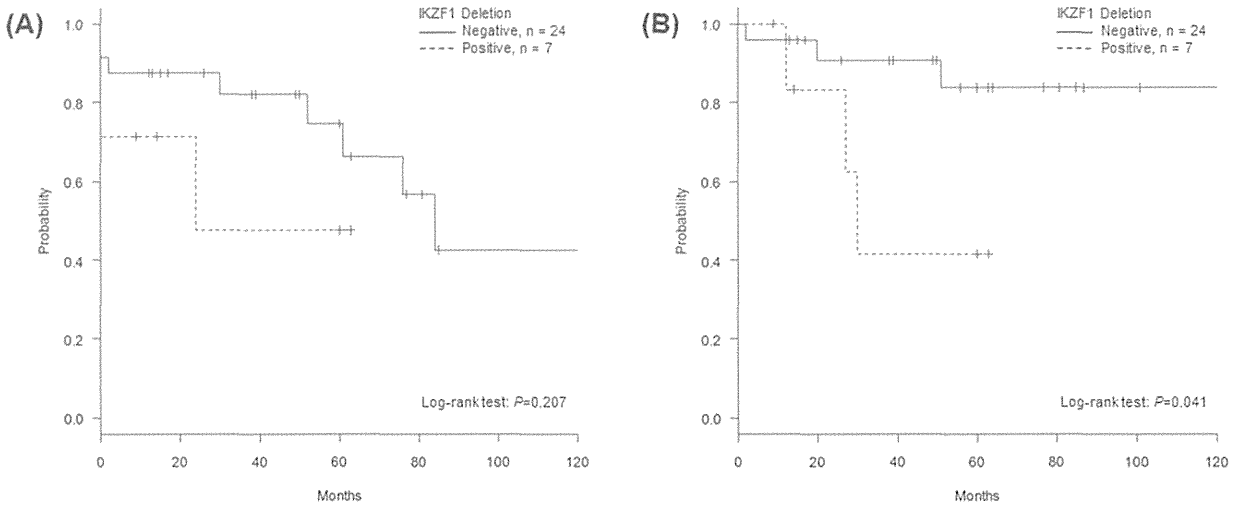

Figure 3. Clinical outcome of DS-ALL patients according to *IKZF1* deletions. (A) Event-free survival. (B) Overall survival.

alteration, with the exception of inferior OS in patients with *IKZF1* deletions (41.7 ± 22.2% vs. 83.8 ± 8.9% at 5 years, $P = 0.041$; Table 2 and Fig. 3).

DISCUSSION

In this study, the frequency of *P2RY8-CRLF2* in Japanese DS-ALL patients was slightly lower (29%) than that in Western countries (~50%), a finding that was confirmed by MLPA. Initially, the frequency of *P2RY8-CRLF2* was thought to be 21% (8/38), but three additional patients, none of whom had available RNA samples, were positive for *P2RY8-CRLF2* by genomic PCR using primer sets that detected the newly discovered *CRLF2* breakpoints (Morak et al., 2012). These primer sets should be included in genomic PCR analysis to avoid an underestimation of the frequency of *P2RY8-CRLF2*.

We could not investigate the *IGH-CRLF2* rearrangement because samples for fluorescence in situ hybridization analysis were not available. Instead, we studied *CRLF2* expression levels in DS-ALL and non-DS ALL patients, as *CRLF2* expression levels are higher in *IGH-CRLF2*-positive DS-ALL patients than in *P2RY8-CRLF2*-positive DS-ALL patients (Russell et al., 2009; Harvey et al., 2010). However, no significant difference in *CRLF2* expression levels was observed between *P2RY8-CRLF2*-negative DS-ALL and non-DS-ALL patients. Moreover, *CRLF2* overexpression was observed in only 3 of 20 *P2RY8-CRLF2*-negative DS-ALL patients. These results suggest that *IGH-CRLF2* is rare in our cohort. The *CRLF2* F232C mutation, which is also associated with *CRLF2* overexpression, was not found in any of the patients. Taken together, these findings suggest that the frequency of *CRLF2* rearrangements including *P2RY8-CRLF2*, *IGH-CRLF2*, and *CRLF2* mutations are lower in DS-ALL patients in Japan than in Western countries.

It is unclear why *CRLF2* rearrangements are less frequent in Japan. One study reported that *CRLF2* rearrangements were associated with Hispanic/Latino ethnicity in a high risk non-DS ALL cohort (Harvey et al., 2010), and two recent studies showed that *P2RY8-CRLF2* and *JAK2* mutations are rare in Japanese non-DS ALL patients (Asai et al., 2013; Yamashita et al., 2013). These results suggest that the frequency of these genetic alterations is dependent on ethnicity.

EBF1 deletions are very rare in DS-ALL patients in Western countries. Three studies did not find *EBF1* deletions in 10, 50, and 34 DS-ALL patients (0%; Ensor et al., 2011; Loudin et al., 2011; Buitenkamp et al., 2012). In two earlier studies, *EBF1* deletions were only detected in 1/9 (11%; Kearney et al., 2009) and 1/15 DS-ALL patients (6.7%; Hertzberg et al., 2010). When these data are combined, the incidence of *EBF1* deletions is 2/118 (1.7%). However, a high frequency of *EBF1* deletions (5/32, 16%) were found in Japanese DS-ALL patients. Therefore, the frequency of *EBF1* deletions may also be dependent on ethnicity.

Moreover, *EBF1* deletions were significantly associated with *P2RY8-CRLF2*. *IKZF1* deletions are associated with *BCR-ABL* and other fusion genes that constitutively activate signaling pathways in *BCR-ABL*-positive ALL and *BCR-ABL*-like ALL, two pathways that are thought to contribute to leukemogenesis (Mullighan et al., 2008; Roberts et al., 2012). In the same manner, *EBF1* deletions and *P2RY8-CRLF2* may act to induce leukemogenesis in a subset of Japanese DS-ALL patients. Conversely, deletions of *CDKN2A/B* and *PAX5* were common in *P2RY8-CRLF2*-negative patients but rare in *P2RY8-CRLF2*-positive patients. It has been reported that *IKZF1* deletions are not associated with *P2RY8-CRLF2* or *JAK2* mutations in DS-ALL (Buitenkamp et al., 2012), but other associations with gene alterations remains unclear.

BTG1 deletions were detected in 8 of 32 patients (25%), with a frequency similar to that of Lundin et al. (2012) (29%) and higher than that of Buitenkamp et al. (2013) (6.9%). However, we could not confirm the previously reported associations of *BTG1* deletions with male predominance and older age (Lundin et al., 2012). *IKZF1* deletions were observed in 8 of 32 patients (25%) with a frequency similar to those in previous reports (Buitenkamp et al., 2012; Patrick et al., 2014). Although the number of patients was limited, estimated OS was significantly shorter in patients with *IKZF1* deletions, which is also consistent with previous reports (Buitenkamp et al., 2012; Patrick et al., 2014). To determine the exact frequencies and clinical implications of these deletions in Japanese DS-ALL patients will require the evaluation of more patients.

In conclusion, a relatively low frequency of *P2RY8-CRLF2*, a high frequency of *EBF1* deletions, and an association of *EBF1* deletions and *P2RY8-CRLF2* were found in Japanese DS-ALL patients. The results indicate that differences exist between the genetic profiles of DS-ALL patients in Japan and in Western countries, and that *P2RY8-CRLF2* and *EBF1* deletions may cooperate in leukemogenesis in a subset of Japanese DS-ALL patients. Further studies are needed to characterize the full spectrum of genetic alterations in Japanese DS-ALL patients and to identify a potential target for therapy.

ACKNOWLEDGMENTS

The authors thank Hirokazu Kanegane, University of Toyama; Akitoshi Kinoshita, St. Marianna University School of Medicine; Kazutaka Takaki, National Hospital Organization Kumamoto Medical Center; and Satoshi Saida and Hidefumi Hiramatsu, Kyoto University for providing patient samples and data. The authors also thank RuNan Wang and Hisae Kudo for their technical assistance.

REFERENCES

Asai D, Imamura T, Suenobu S, Saito A, Hasegawa D, Deguchi T, Hashii Y, Matsumoto K, Kawasaki H, Hori H, Iguchi A, Kosaka Y, Kato K, Horibe K, Yumura-Yagi K, Hara J, Oda M;

Japan Association of Childhood Leukemia Study (JACLS). 2013. *IKZF1* deletion is associated with a poor outcome in pediatric B-cell precursor acute lymphoblastic leukemia in Japan. Cancer Med 2:412–419.

Bercovich D, Ganmore I, Scott LM, Wainreb G, Birger Y, Elimelech A, Shochat C, Cazzaniga G, Biondi A, Basso G, Cario G, Schrappe M, Stanulla M, Strehl S, Haas OA, Mann G, Binder V, Borkhardt A, Kempski H, Trka J, Bielorei B, Avigad S, Stark B, Smith O, Dastugue N, Bourquin JP, Tal NB, Green AR, Izraeli S. 2008. Mutations of *JAK2* in acute lymphoblastic leukaemias associated with Down's syndrome. Lancet 372: 1484–1492.

Blink M, Buitenkamp TD, van den Heuvel-Eibrink MM, Danen-van Oorschot AA, de Haas V, Reinhardt D, Klusmann JH, Zimmermann M, Devidas M, Carroll AJ, Basso G, Pession A, Hasle H, Pieters R, Rabin KR, Izraeli S, Zwaan CM. 2011. Frequency and prognostic implications of *JAK 1–3* aberrations in Down syndrome acute lymphoblastic and myeloid leukemia. Leukemia 25:1365–1368.

Buitenkamp TD, Pieters R, Gallimore NE, van der Veer A, Meijerink JP, Beverloo HB, Zimmermann M, de Haas V, Richards SM, Vora AJ, Mitchell CD, Russell LJ, Schwab C, Harrison CJ, Moorman AV, van den Heuvel-Eibrink MM, den Boer ML, Zwaan CM. 2012. Outcome in children with Down's syndrome and acute lymphoblastic leukemia: Role of *IKZF1* deletions and *CRLF2* aberrations. Leukemia 26:2204–2211.

Buitenkamp TD, Pieters R, Zimmermann M, de Haas V, Richards SM, Vora AJ, Mitchell CD, Schwab C, Harrison CJ, Moorman AV, van den Heuvel-Eibrink MM, Zwaan CM. 2013. *BTG1* deletions do not predict outcome in Down syndrome acute lymphoblastic leukemia. Leukemia 27:251–252.

Buitenkamp TD, Izraeli S, Zimmermann M, Forestier E, Heerema NA, van den Heuvel-Eibrink MM, Pieters R, Korbijn CM, Silverman LB, Schmiegelow K, Liang DC, Horibe K, Arico M, Biondi A, Basso G, Rabin KR, Schrappe M, Cario G, Mann G, Morak M, Panzer-Grümayer R, Mondelaers V, Lammens T, Cavé H, Stark B, Ganmore I, Moorman AV, Vora A, Hunger SP, Pui CH, Mullighan CG, Manabe A, Escherich G, Kowalczyk JR, Whitlock JA, Zwaan CM. 2014. Acute lymphoblastic leukemia in children with Down syndrome: A retrospective analysis from the Ponte di Legno study group. Blood 123:70–77.

Ensor HM, Schwab C, Russell LJ, Richards SM, Morrison H, Masic D, Jones L, Kinsey SE, Vora AJ, Mitchell CD, Harrison CJ, Moorman AV. 2011. Demographic, clinical, and outcome features of children with acute lymphoblastic leukemia and *CRLF2* deregulation: Results from the MRC ALL97 clinical trial. Blood 117:2129–2136.

Forestier E, Izraeli S, Beverloo B, Haas O, Pession A, Michalová K, Stark B, Harrison CJ, Teigler-Schlegel A, Johansson B. 2008. Cytogenetic features of acute lymphoblastic and myeloid leukemias in pediatric patients with Down syndrome: An iBFM-SG study. Blood 111:1575–1583.

Gaikwad A, Rye CL, Devidas M, Heerema NA, Carroll AJ, Izraeli S, Plon SE, Basso G, Pession A, Rabin KR. 2009. Prevalence and clinical correlates of *JAK2* mutations in Down syndrome acute lymphoblastic leukaemia. Br J Haematol 144: 930–932.

Harvey RC, Mullighan CG, Chen IM, Wharton W, Mikhail FM, Carroll AJ, Kang H, Liu W, Dobbin KK, Smith MA, Carroll WL, Devidas M, Bowman WP, Camitta BM, Reaman GH, Hunger SP, Downing JR, Willman CL. 2010. Rearrangement of *CRLF2* is associated with mutation of *JAK* kinases, alteration of *IKZF1*, Hispanic/Latino ethnicity, and a poor outcome in pediatric B-progenitor acute lymphoblastic leukemia. Blood 115: 5312–5321.

Hertzberg L, Vendramini E, Ganmore I, Cazzaniga G, Schmitz M, Chalker J, Shiloh R, Iacobucci I, Shochat C, Zeligson S, Cario G, Stanulla M, Strehl S, Russell LJ, Harrison CJ, Bornhauser B, Yoda A, Rechavi G, Bercovich D, Borkhardt A, Kempski H, te Kronnie G, Bourquin JP, Domany E, Izraeli S. 2010. Down syndrome acute lymphoblastic leukemia, a highly heterogeneous disease in which aberrant expression of *CRLF2* is associated with mutated *JAK2*: A report from the International BFM Study Group. Blood 115:1006–1017.

Kearney L, Gonzalez De Castro D, Yeung J, Procter J, Horsley SW, Eguchi-Ishimae M, Bateman CM, Anderson K, Chaplin T, Young BD, Harrison CJ, Kempski H, So CW, Ford AM, Greaves M. 2009. Specific *JAK2* mutation (*JAK2*R683) and multiple gene deletions in Down syndrome acute lymphoblastic leukemia. Blood 113:646–648.

Loudin MG, Wang J, Leung HC, Gurusiddappa S, Meyer J, Condos G, Morrison D, Tsimelzon A, Devidas M, Heerema NA, Carroll AJ, Plon SE, Hunger SP, Basso G, Pession A, Bhojwani D, Carroll WL, Rabin KR. 2011. Genomic profiling in Down syndrome acute lymphoblastic leukemia identifies histone gene deletions associated with altered methylation profiles. Leukemia 25:1555–1563.

Lundin C, Hjorth L, Behrendtz M, Nordgren A, Palmqvist L, Andersen MK, Biloglav A, Forestier E, Paulsson K, Johansson B. 2012. High frequency of *BTG1* deletions in acute lymphoblastic leukemia in children with Down syndrome. Genes Chromosomes Cancer 51:196–206.

Maloney KW, Carroll WL, Carroll AJ, Devidas M, Borowitz MJ, Martin PL, Pullen J, Whitlock JA, Willman CL, Winick NJ, Camitta BM, Hunger SP. 2010. Down syndrome childhood acute lymphoblastic leukemia has a unique spectrum of sentinel cytogenetic lesions that influences treatment outcome: A report from the Children's Oncology Group. Blood 116:1045–1050.

Morak M, Attarbaschi A, Fischer S, Nassimbeni C, Grausenburger R, Bastelberger S, Krentz S, Cario G, Kasper D, Schmitt K, Russell LJ, Pötschger U, Stanulla M, Eckert C, Mann G, Haas OA, Panzer-Grümayer R. 2012. Small sizes and indolent evolutionary dynamics challenge the potential role of *P2RY8-CRLF2*-harboring clones as main relapse-driving force in childhood ALL. Blood 120:5134–5142.

Mullighan CG, Miller CB, Radtke I, Phillips LA, Dalton J, Ma J, White D, Hughes TP, Le Beau MM, Pui CH, Relling MV, Shurtleff SA, Downing JR. 2008. *BCR-ABL1* lymphoblastic leukaemia is characterized by the deletion of Ikaros. Nature 453: 110–114.

Mullighan CG, Collins-Underwood JR, Phillips LA, Loudin MG, Liu W, Zhang J, Ma J, Coustan-Smith E, Harvey RC, Willman CL, Mikhail FM, Meyer J, Carroll AJ, Williams RT, Cheng J, Heerema NA, Basso G, Pession A, Pui CH, Raimondi SC, Hunger SP, Downing JR, Carroll WL, Rabin KR. 2009. Rearrangement of *CRLF2* in B-progenitor- and Down syndrome-associated acute lymphoblastic leukemia. Nat Genet 41: 1243–1246.

Nižetić D, Groet J. 2012. Tumorigenesis in Down's syndrome: Big lessons from a small chromosome. Nat Rev Cancer 12:721–732.

Patrick K, Wade R, Goulden N, Rowntree C, Hough R, Moorman AV, Mitchell CD, Vora A. 2014. Outcome of Down syndrome associated acute lymphoblastic leukaemia treated on a contemporary protocol. Br J Haematol 165:552–555.

Roberts KG, Morin RD, Zhang J, Hirst M, Zhao Y, Su X, Chen SC, Payne-Turner D, Churchman ML, Harvey RC, Chen X, Kasap C, Yan C, Becksfort J, Finney RP, Teachey DT, Maude SL, Tse K, Moore R, Jones S, Mungall K, Birol I, Edmonson MN, Hu Y, Buetow KE, Chen IM, Carroll WL, Wei L, Ma J, Kleppe M, Levine RL, Garcia-Manero G, Larsen E, Shah NP, Devidas M, Reaman G, Smith M, Paugh SW, Evans WE, Grupp SA, Jeha S, Pui CH, Gerhard DS, Downing JR, Willman CL, Loh M, Hunger SP, Marra MA, Mullighan CG. 2012. Genetic alterations activating kinase and cytokine receptor signaling in high-risk acute lymphoblastic leukemia. Cancer Cell 22:153–166.

Russell LJ, Capasso M, Vater I, Akasaka T, Bernard OA, Calasanz MJ, Chandrasekaran T, Chapiro E, Gesk S, Griffiths M, Guttery DS, Haferlach C, Harder L, Heidenreich O, Irving J, Kearney L, Nguyen-Khac F, Machado L, Minto L, Majid A, Moorman AV, Morrison H, Rand V, Strefford JC, Schwab C, Tönnies H, Dyer MJ, Siebert R, Harrison CJ. 2009. Deregulated expression of cytokine receptor gene, *CRLF2*, is involved in lymphoid transformation in B-cell precursor acute lymphoblastic leukemia. Blood 114:2688–2698.

Sato T, Toki T, Kanezaki R, Xu G, Terui K, Kanegane H, Miura M, Adachi S, Migita M, Morinaga S, Nakano T, Endo M, Kojima S, Kiyoi H, Mano H, Ito E. 2008. Functional analysis of *JAK3* mutations in transient myeloproliferative disorder and acute megakaryoblastic leukaemia accompanying Down syndrome. Br J Haematol 141:681–688.

Schwab CJ, Jones LR, Morrison H, Ryan SL, Yigittop H, Schouten JP, Harrison CJ. 2010. Evaluation of multiplex ligation-dependent probe amplification as a method for the detection of copy number abnormalities in B-cell precursor

acute lymphoblastic leukemia. Genes Chromosomes Cancer 49: 1104–1113.

Shochat C, Tal N, Bandapalli OR, Palmi C, Ganmore I, te Kronnie G, Cario G, Cazzaniga G, Kulozik AE, Stanulla M, Schrappe M, Biondi A, Basso G, Bercovich D, Muckenthaler MU, Izraeli S. 2011. Gain-of-function mutations in *interleukin-7 receptor-α* (*IL7R*) in childhood acute lymphoblastic leukemias. J Exp Med 208:901–908.

Yamashita Y, Shimada A, Yamada T, Yamaji K, Hori T, Tsurusawa M, Watanabe A, Kikuta A, Asami K, Saito AM, Horibe K. 2013. *IKZF1* and *CRLF2* gene alterations correlate with poor prognosis in Japanese *BCR-ABL1*-negative high-risk B-cell precursor acute lymphoblastic leukemia. Pediatr Blood Cancer 60:1587–1592.

Yoda A, Yoda Y, Chiaretti S, Bar-Natan M, Mani K, Rodig SJ, West N, Xiao Y, Brown JR, Mitsiades C, Sattler M, Kutok JL, DeAngelo DJ, Wadleigh M, Piciocchi A, Dal Cin P, Bradner JE, Griffin JD, Anderson KC, Stone RM, Ritz J, Foà R, Aster JC, Frank DA, Weinstock DM. 2010. Functional screening identifies CRLF2 in precursor B-cell acute lymphoblastic leukemia. Proc Natl Acad Sci USA 107:252–257.

Pediatr Blood Cancer 2014;61:1257–1262

Prognostic Factors of Epstein–Barr Virus-Associated Hemophagocytic Lymphohistiocytosis in Children: Report of the Japan Histiocytosis Study Group

Kazuhiro Kogawa, MD, PhD,[1,2]* Hiroki Sato, MS,[3] Takeshi Asano, MD, PhD,[2] Shouichi Ohga, MD, PhD,[2] Kazuko Kudo, MD, PhD,[2] Akira Morimoto, MD, PhD,[2] Shigeru Ohta, MD, PhD,[2] Hiroshi Wakiguchi, MD, PhD,[2] Hirokazu Kanegane, MD, PhD,[4] Megumi Oda, MD, PhD,[4] and Eiichi Ishii, MD, PhD[2]

Background. Despite several advances in the treatment of Epstein–Barr virus (EBV) in recent years, patients with Epstein–Barr virus-associated hemophagocytic lymphohistiocytosis (EBV-HLH) do not always show satisfactory outcomes. We here conducted a nationwide survey in Japan to identify prognostic factors of EBV-HLH in children with this disease in an effort to improve the management and the outcomes of these patients. ***Procedure.*** Between January 2003 and June 2008, we enrolled 98 children younger than 18 years of age who were diagnosed with EBV-HLH. We then studied the clinical characteristics and laboratory findings at the time of diagnosis with the aim to identify prognostic factors for EBV-HLH. ***Results.*** The mean age of onset of EBV-HLH was 3.9 ± 2.8 years. Most of our patients presented with fever, hepatosplenomegaly, lymphadenopathy, and hemophagocytosis of bone marrow. Sixty-two percent of patients showed T cell clonality, and 97% had EBV infection in either T or natural killer cells. Most patients (60%) were treated with a multi-agent chemotherapeutic regimen, including corticosteroid, etoposide, and cyclosporine. After initial treatment, 90.3% of patients were in remission, and 7 patients (8.2%) experienced recurrence of EBV infection. Among several prognostic factors, patients with both hyperbilirubinemia (>1.8 mg/dl) and hyperferritinemia (>20,300 ng/ml) at the time of diagnosis had significantly poorer outcomes than those with low serum bilirubin and ferritin levels. ***Conclusions.*** These findings suggest that the therapeutic strategy for children with EBV-HLH could be tailored according to the laboratory findings at diagnosis. Pediatr Blood Cancer 2014;61:1257–1262.

Key words: Epstein–Barr virus; Epstein–Barr virus-associated hemophagocytic lymphohistiocytosis; hyperbilirubinemia; hyperferritinemia

INTRODUCTION

Hemophagocytic lymphohistiocytosis (HLH) is an immune disorder characterized by fever, hepatosplenomegaly, pancytopenia, hypertriglyceridemia, and hypofibrinogenemia, and patients with HLH often experience seizures [1]. HLH can be classified as either primary or secondary HLH. Epstein–Barr virus (EBV) infection is known to induce secondary HLH in some patients, and Epstein–Barr virus-associated HLH (EBV-HLH) is considered a major subtype of secondary HLH [2]. It is difficult to distinguish between primary and secondary HLH based on clinical symptoms, history of infection, or the early clinical course at the onset of disease. Distinguishing between primary and secondary HLH is further complicated by the fact that EBV infection can also trigger primary HLH [3].

Although not all countries have known incidence rates for EBV-HLH, this disease is thought to be particularly prevalent in Asian countries [4]. A nationwide survey of HLH in Japan estimated the annual incidence of HLH amongst children and adults at 1 in 800,000 per year. According to this survey, the most common HLH subtype is EBV-HLH, accounting for approximately 40% of all patients with HLH [5].

Prognostic factors for EBV-HLH in children are not yet well described. A number of studies have shown that an EBV infection of T cells or natural killer (NK) cells is associated with an unfavorable prognosis [6,7]. Imashuku et al. [8] reported that treatment with an etoposide within 4 weeks from the diagnosis of HLH improved the prognosis of patients with EBV-HLH. This study also showed that combination-treatment, consisting of etoposide, dexamethasone, and cyclosporine A, can effectively control EBV-HLH [2,9]. A proportion of patients with EBV-HLH spontaneously recovered after supportive therapy only. Spontaneous recoveries have been documented even in patients with severe EBV-HLH [10], and this highlights the difficulty of choosing an appropriate treatment for children who present with EBV-HLH.

DOI 10.1002/pbc.24980
Published online 17 February 2014 in Wiley Online Library (wileyonlinelibrary.com).

The current study investigated the prognostic factors of EBV-HLH in Japanese children in an effort to improve the therapeutic strategies and the outcomes of children with this disease.

DESIGN AND METHODS

Data Collection

We conducted a nationwide survey amongst children younger than 18 years of age who were diagnosed with EBV-HLH between January 2003 and June 2008. Questionnaires were sent to physicians who were members of the Japanese Society of Pediatric Hematology or the Japanese Society of Pediatric Infectious Diseases. Our survey included questions regarding the age of onset of EBV-HLH, the gender of patients, clinical and laboratory

Additional Supporting Information may be found in the online version of this article.

[1]Tsuchiya Children's Hospital, Kuki, Saitama, Japan; [2]HLH/LCH Committees in the Japanese Society of Pediatric Hematology, Tokyo, Japan; [3]Department of Preventive Medicine and Public Health, National Defense Medical College, Tokorozawa, Saitama, Japan; [4]Research/Education Committees in the Japanese Society of Pediatric Infectious Diseases, Tokyo, Japan

Grant sponsor: Ministry of Health, Labour and Welfare of Japan

Conflict of interest: Nothing to declare.

Authors Contribution: KK and EI were the principal investigators and take primary responsibility for the paper. HS, TA, SO, KK, AM, SO, HW, HK, and MO collected and analyzed the data and prepared the manuscript.

*Correspondence to: Kazuhiro Kogawa, Tsuchiya Children's Hospital, 1-6-7 Kukichuou, Kuki, Saitama 346-0003, Japan
E-mail: kkogawa@tsuchiya.or.jp

Received 22 April 2013; Accepted 17 January 2014

findings at the time of diagnosis, initial treatments, and the outcome of patients as noted on the day of the last observation. We also collected information on the viral load before and after initial treatment. Viral loads were measured in the peripheral blood mononuclear cells (PBMCs; shown as copies/μg of DNA) and plasma (copies/ml) as described previously [11]. Lymphocyte subpopulations (CD4+ and C8+ T, CD56+ NK, and CD19+ B cells) were separated and infected cells were identified by quantitative PCR11 or EBER-1 *in situ* hybridization [12], and their clonality for circulating mononuclear cells was analyzed by gene rearrangement of the T cell receptor or terminal repeat assay [13]. In patients with low/deficient NK activity, younger than 2 years, or positive CNS involvements, protein expression with Western blotting or flow cytometers followed by genetic analysis for perforin, Munc13-4 and syntaxin 11 were performed. The expression of Munc18-2 was not analyzed in this study.

Patient Selection

We used the HLH-2004 protocol of Henter et al. [14] as diagnostic criteria to identify patients with EBV-HLH. In total, 142 patients from 55 institutions in Japan were evaluated for EBV-HLH. Twenty patients were excluded because of incomplete information in the questionnaires, and 25 patients were excluded because of clinical characteristics, including a diagnosis of chronic active EBV infection in 7 patients, insufficient diagnostic criteria in 13, and low viral load counts ($<10^3$ copies in the WBCs or whole blood) in 4. The remaining 98 patients were eligible and enrolled in our study (Fig. 1).

Treatment

The selection of the treatment method was left to the medical doctor in this study. Therefore, treatment was varied among the patients according to the severity of disease or treatment response. Some patients were treated with the HLH-2004 treatment protocol, while others were treated without VP16 or with reduced dose of VP16.

We divided patients according to the treatments that they were given as initial therapy: (i) multi-agent chemotherapy including etoposide, corticosteroid, and CSA according to the HLH-2004 protocol 4; (ii) corticosteroid therapy with or without CSA; and (iii) supportive therapy with IVIG.

Statistical Analyses

Clinical and laboratory data of survivors and non-survivors were compared with unpaired t-tests (continuous variables) and with Fisher's exact tests (categorical variables) Data are reported as mean ± SD, or counts and proportion, where appropriate. We used a Cox proportional hazard regression model to identify prognostic factors for EBV-HLH. For this analysis, a cutoff value for each clinical and laboratory parameter was used to divide patients into two subgroups. The optimal cutoff values of the baseline biochemical parameters were selected according to receiver operating characteristic (ROC) analysis. Overall survival (OS) and progression-free survival (PFS) rates were estimated with the Kaplan–Meier method and compared with the log-rank test. OS was defined as the period from the day of disease onset to the day of last observation or all-cause death and PFS was defined as the period

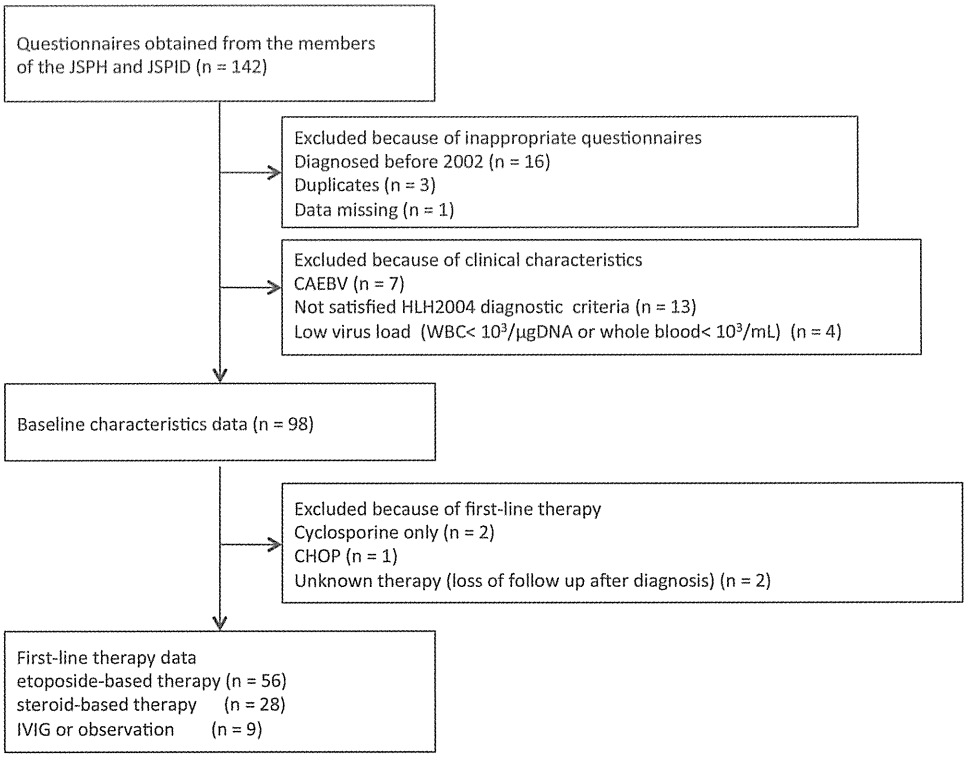

Fig. 1. Selection criteria for the inclusion of EBV-HLH patients in the study.

from the day of disease onset to the day of last observation, death, recurrence after the initial treatment, hematopoietic cell transplantation, or other adverse events (e.g., second malignancy). *P*-values < 0.05 were considered statistically significant. All statistical analyses were performed with SAS version 9.3 (SAS Institute Inc., Cary, NC).

RESULTS

Patient Characteristics and Laboratory Findings

At the onset of EBV-HLH, the mean age of patients was 3.9 ± 2.8 years. The most prominent clinical symptoms were fever (100%), hepatomegaly (87.8%), splenomegaly (64.3%), lymphadenopathy (50.0%), and neurological symptoms as CNS involvement (18.4%). A diagnosis of hemophagocytosis was confirmed in 89 of the 96 assessed patients. Clonality of infected cells was observed in 28 of the 41 tested patients (68.3%). In 33 patients, EBV-infected cells were analyzed, and T cells and/or NK cells and/or B cells were identified in all except one of them. The median EBV load at onset was 1.1×10^5 copies/μg DNA in the WBCs, 1.4×10^6 copies/ml in the plasma, and 5.0×10^5 copies/ml in whole blood. There were no patients with genetic abnormality, shown to be causative of FEL. EBV-HLH observed in this study was simply secondary HLH, which was caused due to EBV infection. In addition, function of cytotoxic T lymphocytes (CTL) was analyzed in 19 patients whose samples were available. CTL activity was not impaired in all these patients with EBV-HLH.

Treatment and Outcomes

Ninety-three of the 98 patients enrolled in our study received one of the possible treatments that we identified in our survey questionnaire. In total, 56 (60%) patients were treated with the HLH-2004 based regimen, 28 (30%) with corticosteroid therapy; and 9 (10%) with supportive/IVIG therapy. After initial treatment, complete remission (CR) was reported in 90% (84/93) of the patients. Most of the patients who failed to achieve remission after initial treatment (8/9 patients) died. Among eight patients who died without remission, seven died within 8 weeks after treatment. A recurrence of EBV-HLH was seen in 7 (8.3%) of the 84 patients who achieved complete remission after initial treatment. All these patients achieved second remission after treatment with a second-line therapy. Among these patients, one patient received hematopoietic cell transplantation. The 3-year OS and PFS rate in all patients were 91.2% and 79.3%, respectively (Fig. 2). There was no significant difference in the OS or PFS rates between the patients with different treatment regimens. However, among 8 died patients, 6 received corticosteroid and etoposide, and the other 2 had received corticosteroid only. Late effects were reported in only one of the patients enrolled in this study. This patient developed acute monoblastic leukemia 5 months after the end of treatment with the HLH-2004 protocol regimen. The total dose of etoposide given to this patient was 3,900 mg/m^2. The patient was subsequently treated with HSCT and achieved complete remission.

Comparison of Clinical and Laboratory Findings Between Survivors and Non-Survivors

We found no significant differences in the following clinical parameters between survivors (n = 90) and non-survivors (n = 8): male/female ratio, age at onset, incidence and duration of fever, duration from onset to diagnosis, size of hepatomegaly or splenomegaly, presence of lymphadenopathy, and CNS involvement (Table I).

A comparison of laboratory data reported significantly higher total bilirubin levels in non-survivors than in survivors (3.1 ± 2.0 mg/dl and 1.5 ± 1.8 mg/dl for non-survivors versus survivors, respectively, $P = 0.016$). Further, the prothrombin time-international normalized ratio (PT-INR) was significantly higher in non-survivors than in survivors (2.0 ± 1.4 and 1.3 ± 0.3 for non-survivors versus survivors, respectively, $P < 0.0001$). None of the other laboratory parameters differed significantly between survivors and non-survivors (Table II).

Outcomes

Patients with a long duration to diagnosis (≥7 days), high neutrophil counts (≥1,700/μl), high PT-INR (≥1.68) or a slow activated partial thromboplastin time (aPTT, ≥69 seconds), high total bilirubin (≥1.8 mg/dl), and high LDH (≥4,310) had significantly poorer outcomes than those with normal results (Table III; Supplemental Figure S1). Prognoses of patients with or

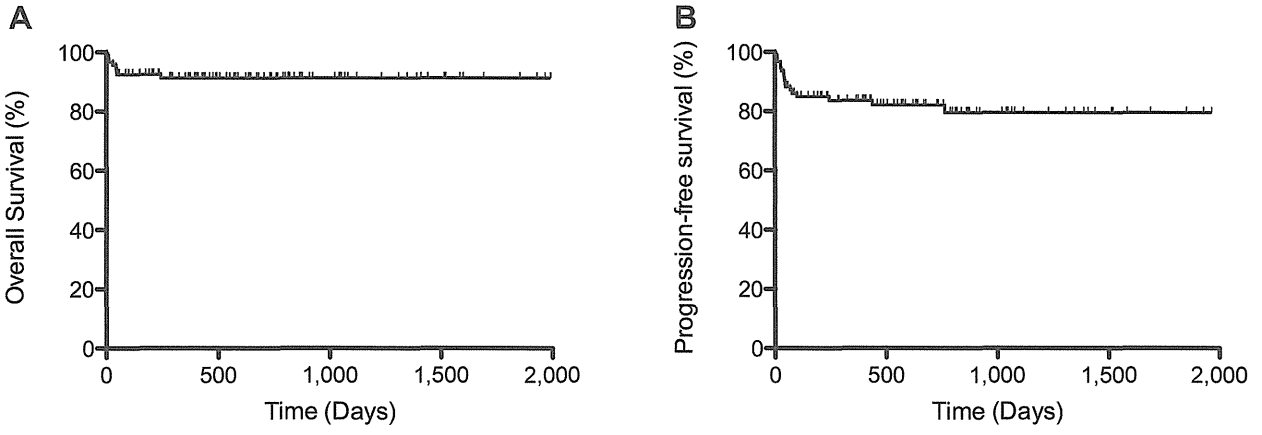

Fig. 2. Overall survival and relapse-free survival (n = 93). **A**: Overall survival of all patients. **B**: Progression-free survival of all patients.

TABLE I. Comparison of Clinical Parameters in Outcome Between the Survived and Died Patients

Characteristics	Survived (n = 90)	Died (n = 8)	*P*-value
Gender[†]			
Male (%)	44 (48.9)	2 (25.0)	0.276
Female (%)	46 (51.1)	6 (75.0)	
Age (years)			
Mean ± SD	3.9 ± 2.8	3.7 ± 1.9	0.847
Duration of fever (days)			
Mean ± SD	8.8 ± 6.0	11.2 ± 5.4	0.374
Duration to diagnosis (days)			
Mean ± SD	7.0 ± 5.9	10.5 ± 5.9	0.111
Splenomegaly (cm)			
Mean ± SD	3.3 ± 1.7	2.3 ± 1.0	0.233
Hepatomegaly (cm)			
Mean ± SD	4.1 ± 2.2	3.9 ± 1.5	0.749
CNS involvements[†]			
Yes (%)	15 (16.7)	3 (37.5)	0.16
No (%)	75 (83.3)	5 (62.5)	
Lymphadenopathy[†]			
Yes (%)	44 (48.9)	5 (62.5)	0.223
No (%)	46 (51.1)	3 (37.5)	

[†]Fisher exact test.

without hyperbilirubinemia (≥1.8 mg/dl) and hyperferritinemia (≥20,300 ng/ml) were significantly different ($P = 0.0038$). One year survival of patients with both hyperbilirubinemia and hyperferritinemia was 0.6923. One year survival of patients without neither hyperbilirubinemia nor hyperferritinemia was 0.9773 (Fig. 3).

DISCUSSION

In our previous study in Japan, more than 40% of the patients with HLH were diagnosed with EBV-HLH, and the annual incidence was estimated at 1 in 800,000 per year [5]. A previous study also estimated that in Japan, the annual incidence of childhood HLH is 51.7 cases per year, and approximately half of these patients have EBV-HLH [15].

We studied the characteristics and laboratory findings of 98 children who contracted EBV-HLH in the 5-year period from January 2003 and June 2008. Because our study encompassed approximately 80% of all patients with EBV-HLH in Japan, the annual incidence of EBV-HLH in children can be estimated at 25 cases per year. However, as the HLH-2004 diagnostic criteria were used for diagnosing EBV-HLH in this study, it is possible that patients with mild type EBV-HLH were overlooked and that the real incidence of EBV-HLH could be higher.

The way in which EBV induces HLH has not been fully elucidated. Su et al. [16] suggested that EBV infection of B cells triggers a polyclonal proliferation of cytotoxic T cells, which is followed by the stimulation of macrophages. This then results in an uncontrolled activation of the immune systems and hypercytokinemia. Data from other studies suggest that EBV targets CD8+ cells or NK cells via the CD21 receptor expressed on these cells. This is thought to trigger a rapid and uncontrolled release of cytokines, and in this way, widespread lymphohistiocytic activation is mediated [17–19]. In addition, impaired function of T cells or NK cells are thought to provide a phenotypic presentation of HLH via any genetic mutation involved in the T/NK cell activation pathway [20,21].

TABLE II. Comparison of Laboratory Parameters in Outcome Between the Survived and Died Patients

	Survived (n = 90)	Died (n = 8)	*P*-value
Hemoglobin (g/dl)			
Mean ± SD	10.0 ± 1.7	8.9 ± 2.2	0.080
Platelet ($\times 10^3/\mu l$)			
Mean ± SD	5.2 ± 2.7	5.1 ± 3.3	0.928
WBC (/μl)			
Mean ± SD	2,561 ± 1,921	2,624 ± 1,455	0.929
Neutrophil (/μl)			
Mean ± SD	829 ± 831	1,046 ± 746	0.505
PT-INR			
Mean ± SD	1.3 ± 0.3	2.0 ± 1.4	<0.0001
aPTT (seconds)			
Mean ± SD	49 ± 30	62 ± 32	0.243
Fibrinogen (mg/dl)			
Mean ± SD	146 ± 71	108 ± 52	0.140
FDP (μg/ml)			
Mean ± SD	49.9 ± 107.6	23.6 ± 22.9	0.554
Tbil (mg/dl)			
Mean ± SD	1.5 ± 1.8	3.1 ± 2.0	0.016
AST (IU/L)			
Mean ± SD	508 ± 814	534 ± 658	0.930
ALT (IU/L)			
Mean ± SD	243 ± 348	230 ± 177	0.916
LDH (IU/L)			
Mean ± SD	2,790 ± 3,001	3,678 ± 4,483	0.445
Tryglyceride (mg/dl)			
Mean ± SD	303 ± 159	410 ± 331	0.124
BUN (mg/dl)			
Mean ± SD	9.8 ± 6.1	10.3 ± 4.2	0.831
Ferritin (ng/ml)			
Mean ± SD	27,820 ± 49,172	45,936 ± 52,839	0.324
sIL-2R (U/ml)			
Mean ± SD	15,904 ± 14,701	26,640 ± 12,203	0.065
NK activity (%)			
Mean ± SD (controls range 18–40%)	24.8 ± 15.4	10.3 ± 11.1	0.117
Hemophagocytosis[†]			
Yes (%)	82 (93.1)	7 (87.5)	0.467
No (%)	6 (6.8)	1 (12.5)	
Not done (%)	2	0	
Clonality[†]			
Yes (%)	28 (68.3)	0 (0.0)	0.049
No (%)	13 (31.7)	0 (0.0)	
Not done (%)	49	8	
EBV-infected cell[†] (T cell or NK cell)			
B cell only (%)	1 (3.4)	0 (0.0)	0.5283
T cell and/or NK and/or B cell (%)	28 (96.6)	4 (100.0)	
Not done (%)	60	4	

[†]Fisher exact test.

EBV-HLH is a heterogeneous disorder with various symptoms that range from mild to severe. In addition, the clinical course of EBV-HLH is diverse and can range from self-limiting in some patients to severe/aggressive and fatal in others. A most appropriate treatment method for EBV-HLH has not yet been established. In

TABLE III. Parameters With Significant Relation to Outcome Before the Start of Therapy (n = 93)

		Crude hazard ratios				Age and sex adjusted hazard ratio			
			95% Confidence interval				95% Confidence interval		
	Cutoff value	Hazard ratio	Lower	Upper	*P*-value	Hazard ratio	Lower	Upper	*P*-value
Duration of fever (days)	11	4.31	0.72	25.86	0.110	4.26	0.70	25.8	0.116
Duration to diagnosis (days)	7	9.10	1.10	75.67	0.041	9.65	1.16	80.49	0.036
Hemoglobin (g/dl)	8.9	0.39	0.10	1.56	0.184	0.29	0.07	1.21	0.089
Platelet ($\times 10^3/\mu l$)	7.1	2.00	0.48	8.37	0.343	2.67	0.62	11.41	0.186
WBC (/μl)	2,400	2.73	0.65	11.43	0.169	2.69	0.63	11.48	0.181
Neutrophil (/μl)	1,700	8.76	1.96	39.19	0.005	9.58	2.05	44.66	0.004
PT-INR	1.68	9.66	2.41	38.75	0.001	11.71	2.83	48.49	0.001
aPTT (seconds)	69	7.71	1.93	30.88	0.004	6.92	1.71	28.00	0.007
Fibrinogen (mg/dl)	149	0.51	0.10	2.53	0.410	0.51	0.10	2.51	0.405
FDP (μg/ml)	16.6	0.47	0.09	2.30	0.348	0.51	0.10	2.54	0.409
Tbil (mg/dl)	1.8	8.62	1.74	42.73	0.008	11.34	2.21	58.30	0.004
AST (IU/L)	474	3.12	0.78	12.49	0.108	3.73	0.92	15.10	0.066
ALT (IU/L)	545	2.07	0.25	16.80	0.497	2.49	0.30	21.00	0.402
LDH (IU/L)	4,310	3.44	0.82	14.41	0.091	4.61	1.04	20.38	0.044
Tryglyceride (mg/dl)	221	3.32	0.40	27.60	0.266	3.23	0.38	27.26	0.282
BUN (mg/dl)	8	3.42	0.41	28.40	0.255	4.17	0.49	35.73	0.193
Ferritin (ng/ml)	20,300	3.69	0.88	15.46	0.074	3.86	0.92	16.23	0.065

this study, more than half of the patients were treated according to the HLH-2004 protocol regimen, whilst 30% received corticosteroid or high-dose γ-globulin and 10% received support care only. Complete remission was achieved in 90% of patients, whilst recurrence was observed in only 8.3% of the patients.

A previous study of patients with EBV-HLH reported that older age (in adults), EBV reactivation, and multidrug chemotherapy were associated with poor clinical outcomes in these patients [5]. We found that in our patients most of the clinical and laboratory parameters, including EBV-load, NK activity EBV-infected cells, and presence of clonality at the onset of disease could not be associated with a poor outcome. Nakazawa et al. showed that change of clonality could be a good marker of disease activity in childhood EBV-HLH [22]. In our limited analysis, at least six patients with EBV-HLH whose EB viral loads remained high after completion of initial therapy have shown long periods of remission, without any further treatment, (Data not shown). In our study, hyperbilirubinemia and hyperferritinemia at the time of diagnosis were significantly associated with a poor outcome. Henter et al. also reported that hyperbilirubinemia and hyperferritinemia at diagnosis, and thrombocytopenia and hyperferritinemia 2 weeks after the initiation of treatment adversely affect the outcome of HLH [23]. Early identification of poor responder to initial treatment based on the clinical or laboratory findings at onset could be benefit for the further improvement of outcome of EBV-HLH. In this study, among eight patients who died without remission, only one patient survived beyond 8 weeks. Therefore, in order to improve the outcome of EBV-HLH, it should be taken into consideration not only to identify poor response but also to control the disease within 8 weeks after treatment.

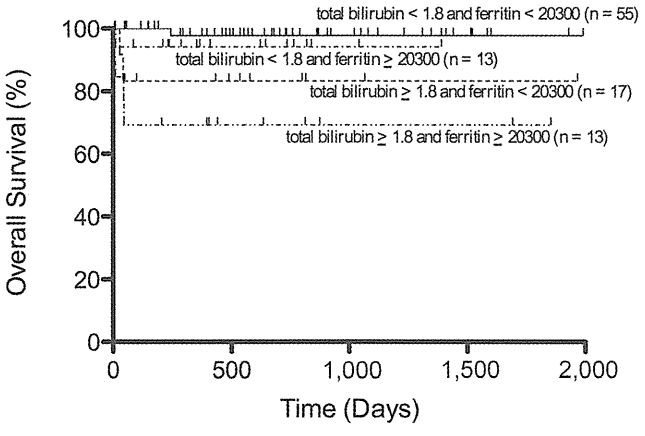

Fig. 3. Overall survival of the four different subgroups classified by the levels of total bilirubin and ferritin.

Huang et al. reported that hypoalbuminemia is an independent predictor for HLH in childhood EBV-associated disease [24]. Taken together, these findings suggest that every patient with EBV-HLH should be treated with a tailored therapeutic strategy based on the laboratory findings at the time of diagnosis. Although it has been reported that hematopoietic stem cell transplantation is an effective treatment for patients with refractory EBV-HLH [25]. The randomized study should be needed to provide evidence that stem cell transplantation could be superior in the outcome of children with EBV-HLH compared to immune-chemotherapy [26].

Balamuth et al. [27] reported that adding rituximab to the HLH-2004 treatment protocol improves the efficacy of the HLH-2004 regimen. Rituximab is a monoclonal antibody directed at CD20, a protein primary found on the surfaces of B cells. Because EBV targets B cells in the initial phase of the disease, rituximab's inhibition of B cells is thought to inhibit the extent of the infection. In addition, B cells may be a target in EBV-associated disease, and rituximab may well be able to reduce morbidity and mortality because it reduces the circulating B cell population and the EB viral load [28]. The anti-thymocyte globulin-based immunotherapy has

also been shown to be an effective treatment for familial HLH. Antithymocyte globulin has an acceptable toxicity level when used as a first-line therapy for familial HLH [29], and this regimen merits investigation as a potential treatment for EBV-infected T cells.

In conclusion, the survival rate of childhood EBV-HLH has improved since the introduction of immunosuppressive therapy in Japan. The reduction of intensity of immunosuppressive therapy must be considered to reduce treatment-related morbidity and mortality in patients without any specific prognostic factors. On the other hand, other small groups of patients with EBV-HLH who show refractory to conventional therapy need stem cell transplantation after receiving standard immunosuppressive therapy. This study suggests that every patient with EBV-HLH must have a tailored treatment strategy which is based on the laboratory findings at the time of diagnosis.

ACKNOWLEDGMENTS

The authors appreciate the coordination provided by all the members of the Japanese Society of Pediatric Hematology and the Japanese Society of Pediatric Infectious Diseases.

REFERENCES

1. Loy TS, Diaz-Arias AA, Perry MC. Familial erythrophagocytic lymphohistiocytosis. Semin Oncol 1991;18:34–38.
2. Imashuku S, Teramura T, Tauchi H, et al. Longitudinal follow-up of patients with Epstein-Barr virus-associated hemophagocytic lymphohistiocytosis. Haematologica 2004;89:183–188.
3. Henter JI, Ehrnst A, Anderson J, et al. Familial hemophagocytic lymphohistiocytosis and viral infection. Acta Paediatr 1993;82:369–372.
4. Janka G, Imashuku S, Elinder G, et al. Infection- and malignancy-associated hemophagocytic syndromes. Secondary hemophagocytic lymphohistiocytosis. Hematol Oncol Clin North Am 1998;12:435–444.
5. Ishii E, Ohga S, Imashuku S, et al. Nationwide survey of hemophagocytic lymphohistiocytosis in Japan. Int J Hematol 2007;86:58–65.
6. Kawaguchi H, Miyashita T, Herbst H, et al. Epstein-Barr virus-infected T lymphocytes in Epstein-Barr virus-associated hemophagocytic syndrome. J Clin Invest 1993;92:1444–1450.
7. Imashuku S, Hibi S, Todo S. Hemophagocytic lymphohistiocytosis in infancy and childhood. J Pediatr 1997;130:352–357.
8. Imashuku S, Kuriyama K, Teramura T, et al. Requirement for etoposide in the treatment of Epstein-Barr virus-associated hemophagocytic lymphohistiocytosis. J Clin Oncol 2001;19:2665–2673.
9. Imashuku S, Hibi S, Ohara T, et al. Effective control of Epstein-Barr virus-related hemophagocytic lymphohistiocytosis with immunochemotherapy. Blood 1999;93:1869–1874.
10. Imashuku I, Teramura T, Kuriyama K, et al. Risk of etoposide-related acute myeloid leukemia in the treatment of Epstein Barr virus-associated hemophagocytic lymphohistiocytosis. Int J Hematol 2002;75: 174–177.
11. Kimura H, Morita M, Yabuta Y, et al. Quantitative analysis of Epstein-Barr virus load by using a real-time PCR assay. J Clin Microbiol 1999;37:132–136.
12. Kasahara Y, Yachie A, Takei K, et al. Differential cellular targets of Epstein-Barr virus (EBV) infection between acute EBV-associated hemophagocytic lymphohistiocytosis and chronic active EBV infection. Blood 2001;98:1882–1888.
13. Imashuku S, Hibi S, Tabata Y, et al. Outcome of clonal hemophagocytic lymphohistiocytosis: Analysis of 32 cases. Leuk Lymphoma 2000;37:577–584.
14. Henter JI, Horne A, Aricó M, et al. HLH-2004: Diagnostic and therapeutic guidelines for hemophagocytic lymphohistiocytosis. Ped Blood Cancer 2007;48:128–131.
15. Imashuku S, Ikushima S, Hibi S, et al. Langerhans cell histiocytosis and hemophagocytic syndrome in Japan: Epidemiological studies. Int J Pediatr Hematol/Oncol 1994;1:241–246.
16. Su IJ, Wang CH, Cheng AL, et al. Hemophagocytic syndrome in Epstein-Barr virus-associated T-lymphoproliferative disorders: Disease spectrum, pathogenesis, and management. Leuk Lymphoma 1995;19:401–406.
17. Moss DJ, Burrows SR, Khanna R, et al. Immune surveillance against Epstein-Barr virus. Semin Immunol 1992;4:97–104.
18. Larroche C, Mouthon L. Pathogenesis of hemophagocytic syndrome (HPS). Autoimmun Rev 2004;3: 69–75.
19. Kasahara Y, Yachie A. Cell type specific infection of Epstein-Barr virus (EBV) in EBV-associated hemophagocytic lymphohistiocytosis and chronic active EBV infection. Crit Rev Oncol Hematol 2002;44:283–294.
20. Nazaruk RA, Rochford R, Hobbs MV, et al. Functional diversity of the CD8 (+) T-cell response to Epstein-Barr virus (EBV): Implications for the pathogenesis of EBV-associated lymphoproliferative disorders. Blood 1998;91:3875–3883.
21. Hatta K, Morimoto A, Ishii E, et al. Association of transforming growth factor-beta1 gene polymorphism in the development of Epstein-Barr virus related hematologic diseases. Haematologica 2007;92: 1470–1474.
22. Matsuda K, Nakazawa Y, Yanagisawa R, et al. Detection of T-cell receptor gene rearrangement in children with Epstein-Barr virus-associated hemophagocytic lymphohistiocytosis using the IOMED-2 multiplex polymerase chain reaction combined with GeneScan analysis. Clin Chim Acta 2011;412: 1554–1558.
23. Trottestam H, Berglöf E, Horne A, et al. Risk factors for early death in children with hemophagocytic lymphohistiocytosis. Acta Paediatr 2012;101:313–318.
24. Huang SC, Chen JS, Cheng CN, et al. Hypoalbuminaemia is an independent predictor for hemophagocytic lymphohistiocytosis. Eur J Haematol 2012;89:417–422.
25. Ohga S, Kudo K, Ishii E, et al. Hematopoietic stem cell transplantation for familial hemophagocytic lymphohistiocytosis and Epstein-Barr virus-associated hemophagocytic lymphohistiocytosis in Japan. Pediatr Blood Cancer 2010;54:299–306.
26. Qin Q, Xie Z, Shen Y, et al. Assessment of immunochemotherapy and stem cell transplantation on EBV-associated hemophagocytic lymphohistiocytosis in children: A systematic review and meta analysis. Eur Rev Med Pharmacol Sci 2012;16:672–678.
27. Balamuth NJ, Nichols KE, Paessler M, et al. Use of rituximab in conjunction with immunosuppressive chemotherapy as a novel therapy for Epstein Barr virus-associated hemophagocytic lymphohistiocytosis. J Pediatr Hematol Oncol 2007;29:569–573.
28. Milone MC, Tsai DE, Hodinka RL, et al. Treatment of primary Epstein-Barr virus infection in patients with X-linked lymphoproliferative disease using B-cell-directed therapy. Blood 2005;105:994–996.
29. Mahlaoui N, Ouachée-Chardin M, de Saint Basile, G, et al. Immunotherapy of familial hemophagocytic lymphohistiocytosis with antithymocyte globulins: A single-center retrospective report of 38 patients. Pediatrics 2007;120:622–628.

nature COMMUNICATIONS

ARTICLE

Received 7 Apr 2014 | Accepted 29 Apr 2014 | Published 4 Jun 2014

DOI: 10.1038/ncomms5004

Ulk1-mediated Atg5-independent macroautophagy mediates elimination of mitochondria from embryonic reticulocytes

Shinya Honda[1], Satoko Arakawa[1], Yuya Nishida[1], Hirofumi Yamaguchi[1], Eiichi Ishii[2] & Shigeomi Shimizu[1]

Macroautophagy is a highly conserved intracellular process responsible for the degradation of subcellular constituents. Macroautophagy was recently suggested to be involved in the removal of mitochondria from reticulocytes during the final stage of erythrocyte differentiation. Although Atg5 and Atg7 are indispensable for macroautophagy, their role in mitochondrial clearance remains controversial. We recently discovered that mammalian cells use conventional Atg5/Atg7-dependent macroautophagy as well as an alternative Unc-51-like kinase 1 (Ulk1)-dependent Atg5/Atg7-independent macroautophagy process. We hypothesized that the latter may be involved in mitochondrial clearance from reticulocytes during erythrocyte differentiation. Here we report that fetal definitive reticulocytes from Ulk1-deficient and Ulk1/Atg5 double-deficient mice retain their mitochondria, whereas the mitochondria are engulfed and digested within autophagic structures in wild-type and Atg5-deficient mice. Mitochondrial retention by Ulk1-deficient reticulocytes is far less marked in primitive and adult definitive reticulocytes. These data indicate that Ulk1-dependent Atg5-independent macroautophagy is the dominant process of mitochondrial clearance from fetal definitive reticulocytes.

[1] Department of Pathological Cell Biology, Medical Research Institute, Tokyo Medical and Dental University, 1-5-45 Yushima, Bunkyo-ku, Tokyo 113-8510, Japan. [2] Department of Pediatrics, Ehime University Graduate School of Medicine, Shitsukawa, Toon, Ehime 791-0295, Japan. Correspondence and requests for materials should be addressed to S.S. (email: shimizu.pcb@mri.tmd.ac.jp).

Macroautophagy is an essential maintenance and protective catabolic process involving the digestion of cellular components and damaged organelles within the lysosomes[1,2]. Macroautophagy occurs constitutively at a low level, but is accelerated by cellular stressors, such as starvation, lack of growth factors and DNA damage. The molecular basis of macroautophagy was extensively studied using autophagy-defective mutant yeasts and mammals[2,3]. It is currently accepted that macroautophagy is driven by >30 autophagy-related proteins (Atgs) conserved from yeasts to mammals[4]. The process of macroautophagy is initiated by the multiprotein complex phosphatidylinositol 3-kinase (PI3K) type III containing Atg6 (also called Beclin1), which promotes membrane invagination[5]. The subsequent elongation and closure of the isolation membrane is mediated by two ubiquitin-like conjugation pathways: the Atg5-Atg12 pathway and the microtubule-associated protein 1 light chain 3 (LC3) pathway[4]. Both pathways depend on the E1-like enzyme Atg7. Thus, several core macroautophagy molecules are believed to be indispensable for macroautophagy, particularly PI3K, Atg5 and Atg7.

We recently discovered that macroautophagy occurs in cells lacking Atg5 and Atg7 (ref. 6). We named this process 'alternative macroautophagy' to distinguish it from Atg5/Atg7-dependent conventional macroautophagy. The role is similar to conventional macroautophagy; whereby, cellular components and organelles are digested within autophagosomes. But the signalling pathway involves PI3K, and not Atg5, Atg7 or LC3. We also found that this pathway is largely dependent on Unc-51-like kinase 1 (Ulk1), a mammalian homologue of yeast Atg1. This kinase is involved in the initiation of conventional macroautophagy and several regulatory mechanisms have been proposed. During starvation, the mTOR complex 1 dissociates from Ulk1, leading to Ulk1 dephosphorylation and activation of the UlK1-Atg13-FIP200-Atg101 complex[7]. In another pathway, Ulk1 is stabilized and activated by the Hsp90-Cdc37 complex[8]. Furthermore, it has been reported that Ulk1 is phosphorylated and acetylated by AMP-activated protein kinase (AMPK)[9] and Tip60 (ref. 10), respectively. All of the above reports were related to the mechanisms by which Ulk1 initiates conventional macroautophagy. However, cells from Ulk1-knockout mice maintained low but significant macroautophagy activity[11]. This study suggests that Ulk1 is not essential for conventional Atg5/Atg7-dependent macroautophagy, but improves the efficiency[11]. This kinase was upregulated during alternative macroautophagy, and Ulk1 silencing markedly inhibited the alternative process[6]. Therefore, Ulk1 may have a dual role, as a facilitator of conventional macroautophagy and as an essential trigger for alternative macroautophagy.

Macroautophagy was previously considered to be a nonselective process, but recent studies demonstrated that distinct macroautophagy signalling pathways regulate the digestion of specific organelles[12,13]. During erythrocyte maturation,

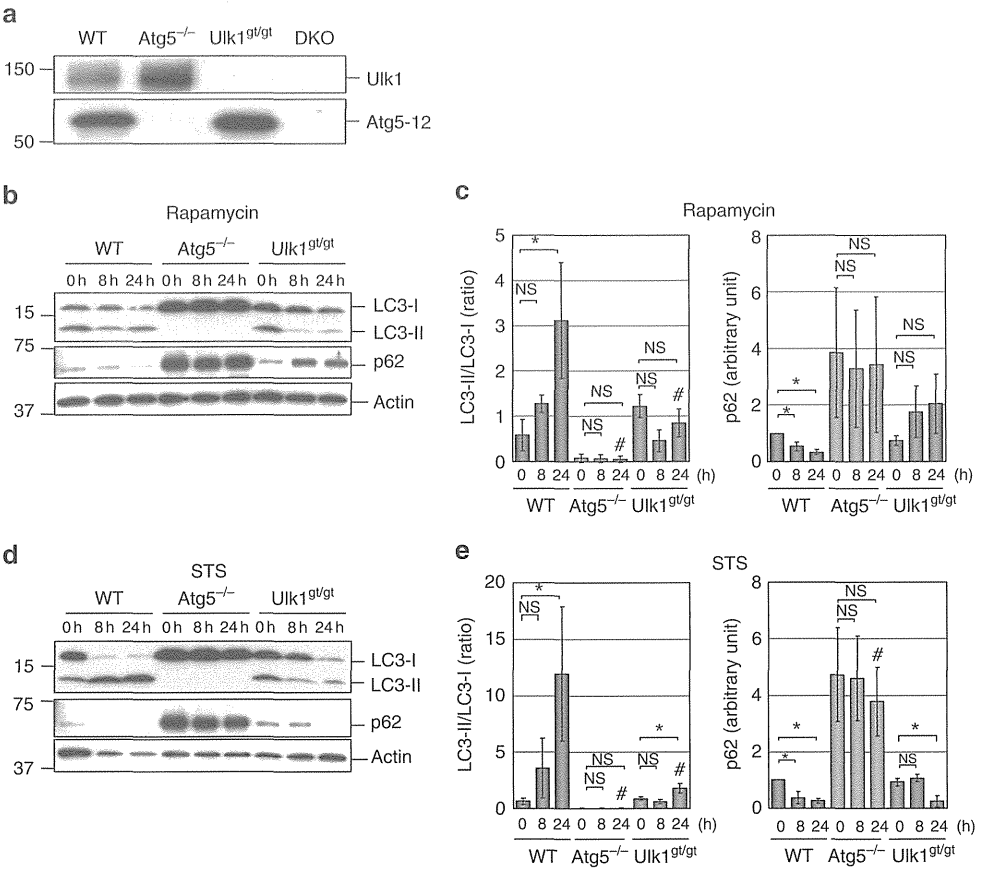

Figure 1 | Induction of conventional macroautophagy in Atg5-deficient erythroid cells by rapamycin and STS. (**a**) Expression of Ulk1 and Atg5-12 in the indicated erythroid cells. (**b**–**e**) Induction of conventional macroautophagy in WT and Ulk1$^{gt/gt}$, but not in Atg5$^{-/-}$, embryonic erythroid cells. Ter119^{+} erythroid cells from WT, Atg5$^{-/-}$, and Ulk1$^{gt/gt}$ embryonic mice (E18.5) were treated with 1 μM rapamycin (**b**,**c**) and 1 μM STS (**d**,**e**), and then harvested at the indicated times. (**b**,**d**) Representative protein expression of LC3 and p62 measured by western blot. Actin was a loading control. Uncropped images are shown in Supplementary Fig. 10. (**c**,**e**) Semi-quantitative analysis of LC3-II/LC3-I and p62 protein expression ($n=3$, mean ± s.d.). Asterisks indicate a significant difference at $P<0.05$ (analysis of variance (ANOVA)). $^{\#}P<0.05$ versus value of WT 24 h (ANOVA). 'NS' indicates not significant (ANOVA).

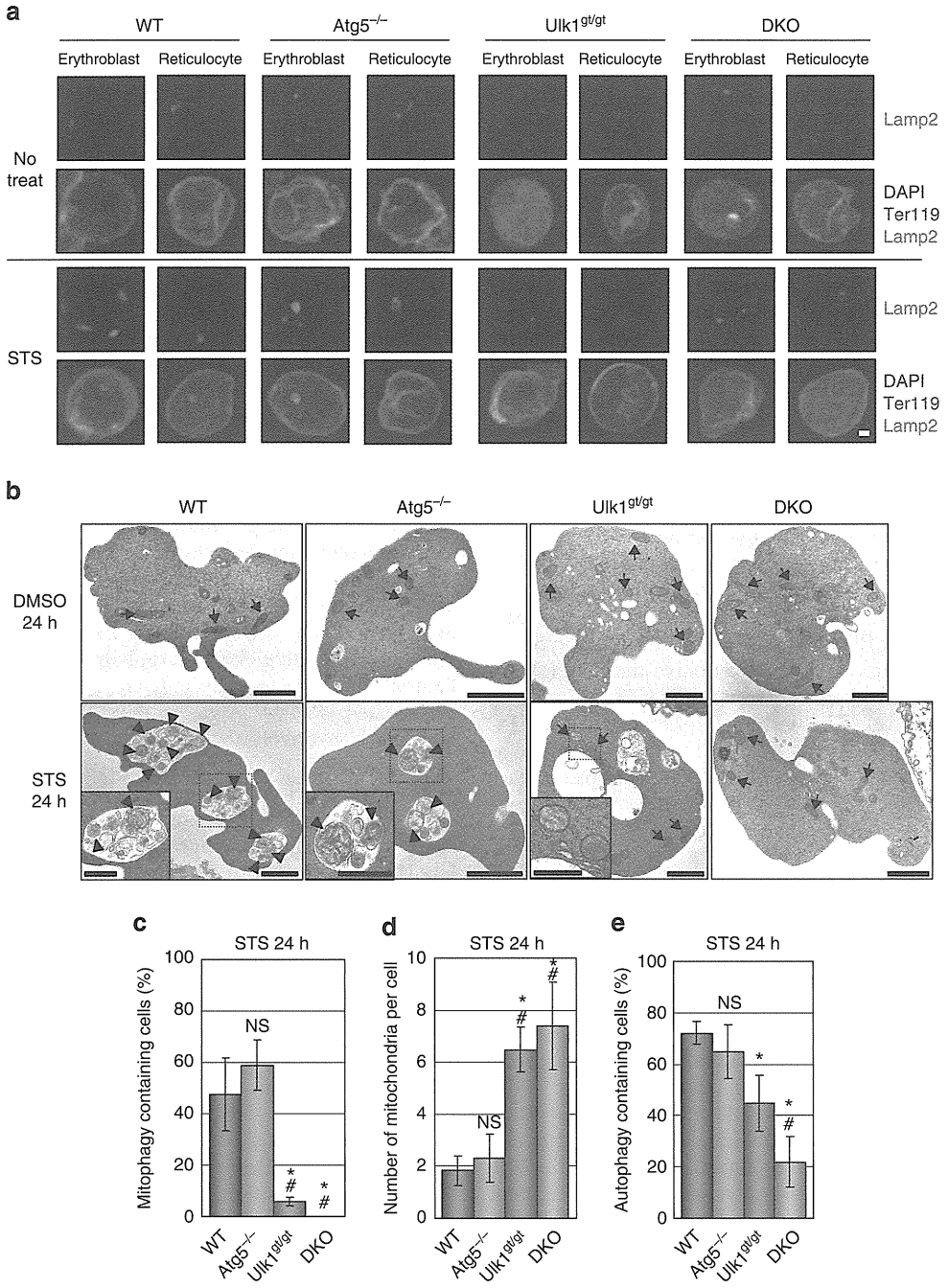

Figure 2 | Induction of alternative macroautophagy in Atg5-deficient erythroid cells by STS. (**a**) Induction of alternative macroautophagy in WT and Atg5$^{-/-}$, but not Ulk1$^{gt/gt}$ and DKO, erythroid cells. Erythroblasts and reticulocytes from the liver of embryonic mice (E18.5) were incubated with or without STS (1 μM) for 24 h, followed by staining with anti-Lamp2 (red), anti-Ter119 (green) and DAPI (blue). DAPI-positive erythroblasts and DAPI-negative reticulocytes are shown. Lamp2 image and merged image (DAPI, Ter119 and Lamp2) are shown. Scale bar, 1 μm. Large dots for Lamp2 are observed in STS-treated WT and Atg5$^{-/-}$ cells, but not STS-treated Ulk1$^{gt/gt}$ or DKO cells. (**b**) Representative electron micrographs of EC incubated with or without STS. Erythroid cells were harvested from the liver of embryonic mice (E18.5), incubated with or without STS (1 μM) for 24 h, and analysed by electron microscopy (EM). Scale bar, 1 μm. Insets of WT and Atg5$^{-/-}$ cells show mitophagy (Scale bar, 0.5 μm). Inset of a Ulk1$^{gt/gt}$ cell showing mitochondria that have not been engulfed (Scale bar, 0.5 μm). Arrows point to non-engulfed mitochondria and the arrowheads indicate engulfed mitochondria. (**c**–**e**) Quantitative analysis of mitophagy after STS treatment, calculated from EM photos. Population of reticulocytes with mitophagy (**c**), number of mitochondria per reticulocytes (**d**) and population of reticulocytes showing macroautophagy (**e**) were calculated ($n>35$ cells per mouse). The data are shown as mean ± s.d. ($n=3$). *$P<0.05$ versus value of WT (analysis of variance (ANOVA)); #$P<0.05$ versus value of Atg5$^{-/-}$ (ANOVA); 'NS' indicates not significant versus value of WT (ANOVA).

the erythroblasts lose their nuclei to become reticulocytes, which are transformed into erythrocytes (EC) by the elimination of organelles, including the mitochondria. It is believed that macroautophagy is involved in this process because ultrastructural studies have detected autophagic structures engulfing mitochondria[14,15]. The involvement of Atg5 and Atg7 remains controversial due to conflicting reports[16–18]. In contrast, Ulk1 has been reported to have an important role[8,11]. Therefore,

we hypothesized that mitochondrial clearance during erythrocyte maturation may be performed by Ulk1-dependent Atg5-independent alternative macroautophagy. This hypothesis was tested by studying mitochondrial clearance from fetal definitive reticulocytes from Ulk1-deficient, Atg5-deficient and Ulk1/Atg5 double-deficient mouse embryos. The contribution of alternative macroautophagy was determined on the basis of the difference between the Atg5-deficient embryos and Ulk1/Atg5 double-deficient embryos. We also determined the weak involvement of Ulk1 in mitochondrial clearance from primitive and adult definitive reticulocytes. Our findings indicate that Ulk1-dependent Atg5-independent macroautophagy is the dominant pathway for mitochondrial clearance from fetal definitive reticulocytes, whereas its role is less important in primitive and adult definitive reticulocytes.

Results

Generation of Ulk1-deficient and Atg5/Ulk1-deficient mice. Ulk1-deficient mice were generated from embryonic stem cells by inserting a gene-trap in *ulk1* (Supplementary Fig. 1a). The absence of Ulk1 protein in the hematopoietic cells of $Ulk1^{gt/gt}$ mice was verified by western blotting (Fig. 1a). The $Ulk1^{gt/gt}$ mice showed mild anaemia (Supplementary Fig. 1b) and splenomegaly (Supplementary Fig. 1c), consistent with the phenotype of $Ulk1^{-/-}$ mice[11]. In addition, Ulk1/Atg5 double-deficient (DKO) mice were generated by crossbreeding $Ulk1^{gt/gt}$ mice with $Atg5^{+/-}$ mice (Fig. 1a). The terminal differentiation of EC proceeded normally in $Ulk1^{gt/gt}$, $Atg5^{-/-}$ and DKO mice, as assessed by the expression of Ter119 and CD71 (Supplementary Fig. 2). These markers were used to identify the different maturation stages of erythroid cells into EC.

Induction of Ulk1-dependent mitophagy by staurosporine. The wild-type (WT), $Ulk1^{gt/gt}$ and $Atg5^{-/-}$ mice were first tested for the presence of functional conventional and/or alternative macroautophagy in cells of the erythroid lineage. The cells were harvested from the liver of embryonic mice on day 18.5 (E18.5) using microbeads conjugated with anti-Ter119 antibodies. The cells were treated with rapamycin to selectively induce conventional (not alternative) macroautophagy[6], and examined for the lipid conjugation of microtubule-associated protein LC3 that occurs during conventional (but not alternative) macroautophagy[6]. LC3-II (a lipid conjugate) was observed in WT cells, but not in $Atg5^{-/-}$ cells, after rapamycin treatment (Fig. 1b,c). Lesser LC3-II formation was detected in $Ulk1^{gt/gt}$ cells than in WT. We also examined the expression of p62, a specific substrate of conventional macroautophagy. Consistent with LC3-II formation, the highest expression of p62 was found in $Atg5^{-/-}$ cells, followed by $Ulk1^{gt/gt}$ and WT cells (Fig. 1b,c). Similar results were obtained when these cells were treated with staurosporine (STS), a pan-kinase inhibitor (Fig. 1d,e). These results show that the lack of Ulk1 expression partially inhibited conventional macroautophagy in erythroid cells.

Conventional and alternative macroautophagy were visualized by confocal microscopy using the non-selective autophagy inducer STS and antibodies against lysosomal-associated membrane protein 2 (Lamp2). Lysosomes are small vesicles distributed throughout the cytosol, so that Lamp2 fluorescence is seen as tiny dots. After the induction of macroautophagy, lysosomes fuse with autophagic vacuoles and the area of Lamp2 fluorescence become much larger. Thus, large Lamp2 fluorescence dots are identical to autolysosomes, as described previously[6]. Small diffuse fluorescent dots were observed in untreated WT erythroid cells, whereas STS-treated WT erythroid cells contained large fluorescent dots (Fig. 2a) suggestive of macroautophagy induction. Large fluorescent dots similar in size and number were observed in STS-treated $Atg5^{-/-}$ erythroid cells. Because conventional macroautophagy was not induced in these cells, the large Lamp2 dots suggest that STS induced alternative macroautophagy. In contrast, fewer large Lamp2 dots were detected in STS-treated $Ulk1^{gt/gt}$ and STS-treated $Ulk1^{gt/gt}$ $Atg5^{-/-}$ DKO erythroid cells, suggesting that Ulk1 is involved in both conventional and alternative macroautophagy.

The two types of macroautophagy were distinguished using anti-LC3 antibodies because this protein only associates with autolysosomes during conventional macroautophagy, and therefore is a good marker to distinguish these two types of autophagic machineries. In this assay, the addition of a lysosomal protease inhibitor (E64d) was required to prevent LC3 degradation in autolysosomes. Selective induction of conventional macroautophagy with rapamycin generated only LC3-positive Lamp2 dots in WT cells (Supplementary Fig. 3). In contrast, STS-treated $Atg5^{-/-}$ cells, where alternative macroautophagy was selectively generated, contained only LC3-negative Lamp2 dots (Supplementary Fig. 3). Expectedly, STS-treated WT and $Ulk1^{gt/gt}$ cells possessed both types of Lamp2 dots. In addition, the size and number of Lamp2 dots was significantly lower in $Ulk1^{gt/gt}$ cells (Supplementary Fig. 3). These findings suggest that STS induces conventional and alternative macroautophagy, both of which are largely dependent on Ulk1.

Figure 3 | Impaired clearance of mitochondria in $Ulk1^{gt/gt}$ and DKO EC. (**a**) Three-colour flow cytometry of erythroid cells from WT embryonic liver (E14.5) stained with anti-Ter119, anti-CD71 and Mitotracker Deep Red. (Left upper panel) Ter119 versus CD71 fluorescence. (Other panels) FSC versus Mitotracker fluorescence of the R1 (right upper panel), R2 (left lower panel) and R3 (right lower panel) fractions. (**b**,**c**) Percentage of cells with a low number of mitochondria (mitochondria^{low} cells) among $CD71^-Ter119^+$ EC. Erythroid cells from the liver (E14.5 and E18.5) and peripheral blood (E18.5) of indicated mice were stained with anti-Ter119, anti-CD71 and Mitotracker Deep Red. (**b**) Representative histograms of mitochondrial content in $CD71^-Ter119^+$ cells. Numbers indicate the population of mitochondria^{low} cells. (**c**) The percentage of $CD71^-Ter119^+$ cells without mitochondria was determined by gating the mitochondria^{low} fraction, as shown in (**b**) (mean ± s.d., $n=6$). $^*P<0.05$ versus value of WT (analysis of variance (ANOVA)); $^{\#}P<0.05$ versus value of $Atg5^{-/-}$ (ANOVA); 'NS' indicates not significant versus value of WT (ANOVA). (**d**) Percent mitochondria^{low} cells in the $CD71^-Ter119^+$ EC of $Atg7^{F/F}$Cre embryo. Erythroid cells from the liver and peripheral blood of WT and $Atg7^{F/F}$Cre embryo (E18.5) were stained with anti-Ter119, anti-CD71, and Mitotracker Deep Red (mean ± s.d., $n=3$). $^*P<0.05$ versus value of WT (Student's *t*-test). (**e**) Percentage of mitochondria^{low} cells in Syto16^{low} cells. Liver erythroid cells (E18.5) were stained with Syto16 (DNA) and Mitotracker Deep Red. Representative dot plots of the mitochondrial content of Syto16^{low} cells are demonstrated in Supplementary Fig. 5, the percentage of Syto16^{low} cells without mitochondria was determined by gating the mitochondria^{low} fraction (mean ± s.d., $n=6$). $^*P<0.05$ versus value of WT (ANOVA); $^{\#}P<0.05$ versus value of $Atg5^{-/-}$ (ANOVA); 'NS' indicates not significant versus value of WT (ANOVA). (**f**) Immunofluorescent analysis of mitochondrial and lysosomal proteins. Liver $Ter119^+$ cells (E18.5) of the indicated mice were stained with anti-Tom20 (mitochondrial marker) and anti-Lamp2 (lysosomal marker) antibodies, and observed by fluorescent microscopy. Scale bar, 2 μm. Green, red, white, and blue indicate Tom20, Lamp2, Ter119 and DAPI (DNA), respectively. Mitochondrial and lysosomal markers have separate distributions in $Ulk1^{gt/gt}$ cells and DKO cells.

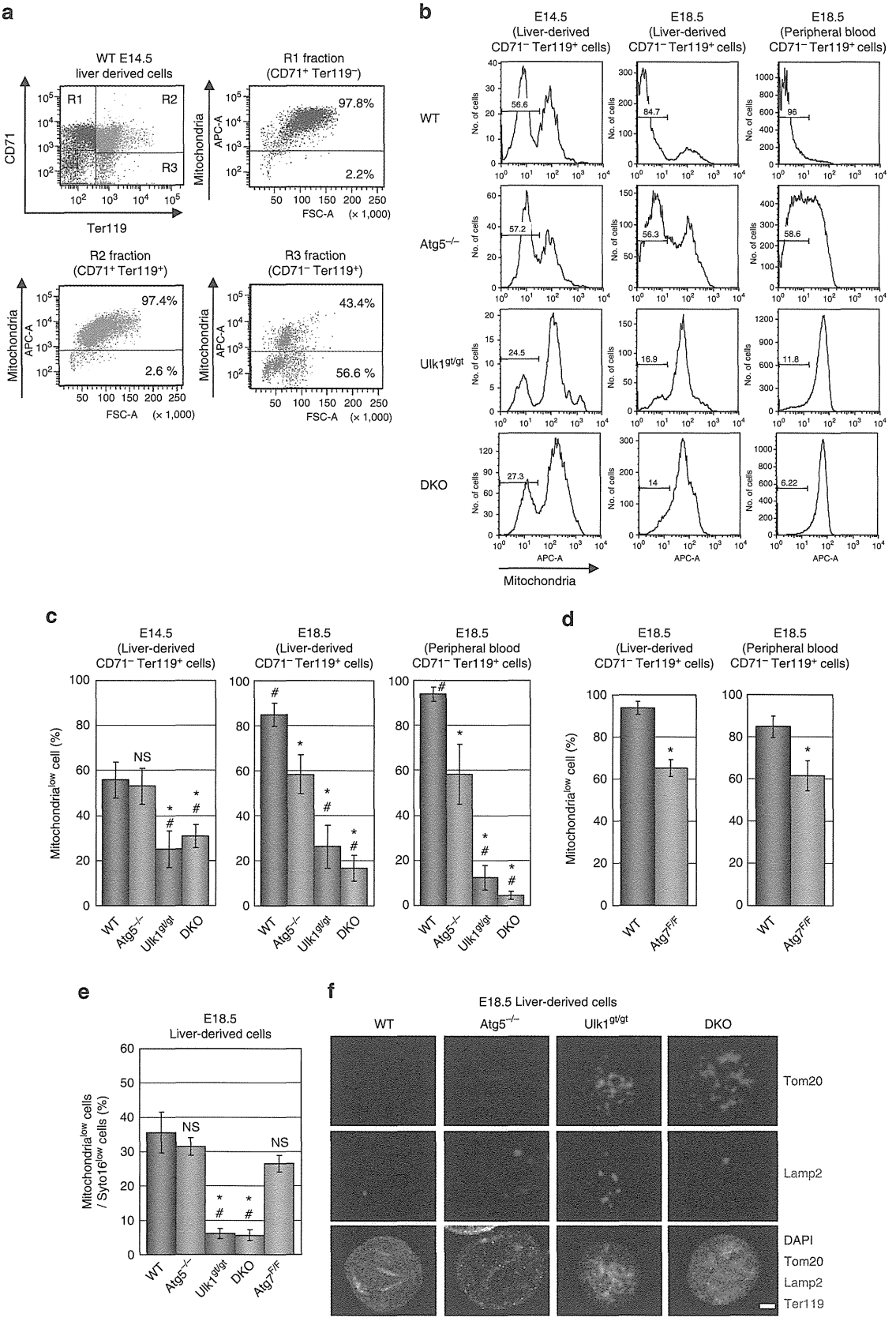

The process of STS-mediated macroautophagy in erythroid cells was further examined by electron microscopy. In WT cells, this exposure caused the formation of several large autophagic vacuoles. The vacuoles engulfed cytoplasmic constituents and mitochondria. Erythroid cells may be unusually susceptible to mitochondrial digestion by macroautophagy ('mitophagy') because this phenomenon was rarely observed in STS-treated embryonic fibroblasts. Similar autophagic vacuoles were observed

in Atg5$^{-/-}$ erythroid cells, but not in DKO erythroid cells (Fig. 2b). Quantitative analysis revealed that mitophagy occurred in about 50% of WT cells and 60% of Atg5$^{-/-}$ cells (Fig. 2c), and the number of mitochondria among these cells was low (Fig. 2d). Autophagic vacuoles were also observed in STS-treated Ulk1$^{gt/gt}$ cells (Fig. 2b,e), but most of them were not used for mitophagy. Thus, the cell population exhibiting mitophagy was small (Fig. 2c), and the number of mitochondria in STS-treated Ulk1$^{gt/gt}$ cells was higher than in STS-treated WT or STS-treated Atg5$^{-/-}$ cells (Fig. 2d). DKO cells contained only a few autophagic vacuoles (Fig. 2b,e), and the mitochondrial numbers were high (Fig. 2d). Although STS is a well-known apoptosis inducer, the apoptotic cell population was low (<25%) under these conditions (Supplementary Fig. 4a). Furthermore, the apoptosis inhibitor Qvd-fmk did not significantly alter the extent of mitochondrial clearance (Supplementary Fig. 4b), indicating that apoptosis was not involved in macroautophagy and mitochondrial clearance. Altogether, these findings indicate that STS induces both conventional and Ulk1-dependent alternative macroautophagy in erythroid cells, and that mitochondria are mainly removed by the latter.

Mitochondrial removal by alternative macroautophagy *in vivo*. Experiments were designed to determine the role of Ulk1-dependent alternative macroautophagy in mitochondrial clearance during erythrocyte differentiation. Hematopoietic ontogeny includes three waves of erythroid lineage: primitive, fetal definitive and adult definitive. The existence of this process in fetal definitive erythroid cells was assessed. Three-colour flow cytometric analysis was conducted using a marker of erythroid precursors (CD71), a marker of late stage erythroid lineage (Ter119) and mitochondria-specific Mitotracker Deep Red staining, indicating that nearly all CD71^{+}Ter119^{-} cells (Fig. 3a left upper panel; R1 fraction) and CD71^{+}Ter119^{+} cells (Fig. 3a left upper panel; R2 fraction) showed strong Mitotracker staining (Fig. 3a right upper and left lower panels) in erythroid cells harvested from the liver of WT embryos on E14.5. In contrast, about 60% of the CD71^{-}Ter119^{+} cells (mature EC) showed weak Mitotracker staining (Fig. 3a left upper panel; R3 fraction, Fig. 3a right lower panel) due to mitochondrial clearance during differentiation. The cell population containing low numbers of mitochondria (mitochondria^{low} cells) among mature Atg5$^{-/-}$ EC (Fig. 3b,c; E14.5 Atg5$^{-/-}$) was equivalent to that of mature WT EC (Fig. 3b,c; E14.5 WT). This population was smaller in Ulk1$^{gt/gt}$ and DKO EC (Fig. 3b,c; E14.5 Ulk1$^{gt/gt}$ and DKO). These data show that erythrocyte differentiation requires Ulk1, but not Atg5, for mitochondrial clearance on E14.5.

In mature EC harvested from the liver and blood on E18.5, most WT cells no longer contained mitochondria (Fig. 3b,c; E18.5 WT), whereas <25% of Ulk1$^{gt/gt}$ and DKO EC had lost their mitochondria (Fig. 3b,c; E18.5 Ulk1$^{gt/gt}$ and DKO), indicating a failure to clear mitochondria in the absence of Ulk1. The mitochondria^{low} population among mature Atg5$^{-/-}$ EC was smaller than that among mature WT EC, but considerably larger than that among Ulk1$^{gt/gt}$ and DKO EC (Fig. 3b,c; E18.5 Atg5$^{-/-}$). Similar results were obtained with hematopoietic-specific Atg7 conditional knockout (Atg7$^{F/F}$;vav1-cre (Atg7$^{F/F}$Cre)) mice (Fig. 3d). These data indicate that Ulk1 plays a predominant role, compared with that of Atg5 and Atg7, in mitochondrial clearance from reticulocytes on E18.5. During erythrocyte differentiation, mitochondria elimination is initiated after enucleation. Therefore, the efficiency of mitochondrial clearance was determined by staining cells with the DNA-specific stain Syto16 and Mitotracker Deep Red. Syto16^{low} cells identified enucleated cells, and the efficiency was calculated from the ratio of mitochondria^{low} Syto16^{low} cells to the total amount of Syto16^{low} cells (Supplementary Fig. 5). The population of mitochondria^{low} Syto16^{low} EC was smaller in Ulk1$^{gt/gt}$ and DKO embryos than in WT, Atg5$^{-/-}$ and Atg7$^{F/F}$Cre embryos (Fig. 3e). These data are consistent with the results obtained by Ter119/CD71/Mitotracker staining (Fig. 3c,d). Furthermore, when late erythroid lineage Ter119-positive cells were immunostained with mitochondria-specific anti-Tom20 antibodies, positive signals were detected in most Ulk1$^{gt/gt}$ and DKO EC, but only in a few WT and Atg5$^{-/-}$ EC (Fig. 3f). Mitochondrial signals rarely merged with Lamp2 fluorescence in Ulk1$^{gt/gt}$ and DKO EC, suggesting that mitophagy did not occur. Altogether, these data indicate that Ulk1 is considerably more important than Atg5 for mitochondrial clearance from reticulocytes during the embryonic period.

The involvement of macroautophagy during the mitochondrial clearance from reticulocytes was further investigated on the basis of ultrastructural changes visualized by EM. On E14.5, the mitochondria was engulfed and digested by autophagic vacuoles in WT reticulocytes (Fig. 4a) and Atg5$^{-/-}$ reticulocytes (Fig. 4b). The cell population exhibiting mitophagy was similar in these two types of reticulocytes (Fig. 4g), whereas mitophagy was largely suppressed in Ulk1$^{gt/gt}$ reticulocytes (Fig. 4c,g). These findings are consistent with the data obtained by flow cytometry (Fig. 3c,e). In DKO reticulocytes, mitophagy was also markedly suppressed, compared with WT reticulocytes (Fig. 4e,g). Accordingly, the number of mitochondria remaining in Ulk1$^{gt/gt}$ and DKO reticulocytes was larger than in WT and Atg5$^{-/-}$ reticulocytes (Fig. 4h). Numerous mitochondria were in contact with the membranous structure in Ulk1$^{gt/gt}$ and DKO reticulocytes. This may indicate that mitochondria were recognized by the isolation membrane, but not enclosed due to the lack of Ulk1. Some of the Ulk1$^{gt/gt}$ and DKO reticulocytes formed plasma membrane blebs and shed cell fragments containing mitochondria (Fig. 4d,f), which may represent a process that removes undigested mitochondria. All these morphological findings support a predominant role for Ulk1-dependent Atg5-independent macroautophagy in the mitochondrial clearance from reticulocytes.

To address the molecular mechanisms of mitophagy during erythrocyte differentiation, erythroblasts (EB; mitochondria^{high} Syto16^{high} cells) and reticulocytes (RC; mitochondria^{high} Syto16^{low} cells) were isolated from embryonic liver using Ter119-conjugated beads, followed by flow cytometric cell sorting. EC (Ter119-positive cells) were also purified from peripheral blood using Ter119-conjugated beads. The expression of key mitochondrial proteins was examined by western blotting. The mitochondrial outer membrane proteins, Tom20 and VDAC, were absent in EC from WT embryos due to mitochondrial clearance. They were detected at low levels in Atg5$^{-/-}$ EC and at high levels in Ulk1$^{gt/gt}$ and DKO EC (Fig. 5a,b). These data confirmed the partial impairment of mitochondrial clearance in Atg5$^{-/-}$ and severe impairment in Ulk1$^{gt/gt}$ and DKO EC. The protein Nix was recently identified as a selective autophagy receptor responsible for mitochondrial clearance from reticulocytes[19–22]. Accordingly, the expression level of Nix in these cell types was proportional to the extent of mitophagy (Fig. 5a,b; EC). Conventional macroautophagy was detected in WT and Ulk1$^{gt/gt}$, but not in Atg5$^{-/-}$ and DKO, erythroblasts and reticulocytes, based on the levels of LC3-II and p62 (Fig. 5a,b). However, this process may not be involved in mitochondrial clearance because mitophagy occurred in Atg5$^{-/-}$ cells where conventional macroautophagy was absent. Furthermore, most signals for LC3 (conventional macroautophagy marker) did not co-localize with Tom20 signals (mitochondria marker) in the erythroblasts and early reticulocytes of WT and Ulk1$^{gt/gt}$ embryos (Supplementary Fig. 6). Therefore, conventional macroautophagy